AMERICAN JOURNAL OF PHYSICAL ANTHROPOLOGY 144:505–515 (2011)

Neandertal Postcranial Remains From the Sima de las Palomas del Cabezo Gordo, Murcia, Southeastern Spain

Michael J. Walker,[1] Jon Ortega,[1] Mariano V. López,[1] Klára Parmová,[1,2] and Erik Trinkaus[3]*

[1]*Área de Antropología Física, Departamento de Zoología y Antropología Física, Facultad de Biología, Campus Universitario de Espinardo, Universidad de Murcia, 30100 Murcia, Spain*
[2]*Laboratory of Biological and Molecular Anthropology, Department of Experimental Biology, Masaryk University, Brno 61137, Czech Republic*
[3]*Department of Anthropology, Washington University, Saint Louis, MO 63130*

KEY WORDS Late Pleistocene; Europe; humerus; femur; ulna; trapezium; phalanx; body proportions; body size

ABSTRACT The Sima de las Palomas, southeastern Spain, has yielded a series of Neandertal postcranial remains, including immature and mature isolated elements and the fragmentary partial skeleton of a young adult (Palomas 92). The remains largely conform to the general late archaic/Neandertal morphological pattern in terms of humeral diaphyseal shape, pectoralis major tuberosity size and pillar thickness, ulnar coronoid process height, manual middle phalangeal epiphyseal breadth, manual distal phalangeal tuberosity shape and breadth, femoral diaphyseal shape, and probably body proportions. Palomas 92 contrasts with the Neandertals in having variably gracile hand remains, a more sellar trapezial metacarpal 1 facet, more anteroposteriorly expanded mid-proximal femoral diaphysis, and less robust pedal proximal phalanges. The Palomas Neandertals contrast with more northern European Neandertals particularly in various reflections of overall body size. Am J Phys Anthropol 144:505–515, 2011.

Since the early descriptions of Neandertal postcranial remains based on the Feldhofer, Spy, La Chapelle-aux-Saints and La Ferrassie remains, descriptions of marine isotope stage (MIS) 4-3 Neandertal postcranial morphology, functional anatomy, body size and body proportions have been dominated by considerations of European Neandertal remains from north of the Pyrenees and the Alps. These discussions have been augmented by Neandertal postcranial remains from the eastern Mediterranean littoral, the Crimea and the Zagros Mountains, plus isolated elements from elsewhere. Yet, assessments of European Neandertal postcrania and especially its geographical variation have been limited by a dearth of European Mediterranean MIS 4-3 postcrania. Such Mediterranean axial and appendicular elements include only the fragmentary remains from Cova Negra, Fate, Oliveira, Santa Croce, and Zafarraya (Cardini, 1955; Giacobini and Lumley, 1988; Barroso-Ruíz et al., 2003; Trinkaus et al., 2007; Arsuaga et al., 2007) and now the Sima de las Palomas (Walker et al., 2008).

It is in this context that we present the Neandertal postcrania from the Sima de las Palomas del Cabezo Gordo, Torre Pacheco, Murcia, southeastern Spain. One salient characteristic of the chronologically late elements of this postcranial sample has been provided (Walker et al., 2008), but they are largely undescribed. They provide the largest sample of both isolated and associated Neandertal postcrania known from Mediterranean Europe, and they raise questions as to whether there was geographical variation in the postcrania similar to that which has been proposed (e.g., Hambücken, 1997; Rosas et al., 2006; Fabre et al., 2009) for Neandertal craniofacial and arm remains.

THE PALOMAS POSTCRANIAL SAMPLE

The postcrania

The Palomas Neandertal postcrania consists of 17 isolated elements (Supporting Information Table S1) plus 45 elements of an associated skeleton (Palomas 92; Supporting Information Table S2) (see Supporting Information for preservation details). In the former sample, only the three phalanges are complete. The other elements are partial but have minimal surface erosion, and none of them is distorted. As such, they provide

Additional Supporting Information may be found in the online version of this article.

Grant sponsor: Spanish Government Research Grants; Grant numbers: CGL2005/02410/BTE, BOS/2002/02375, PB/98/0405, PB/92/0971; Grant sponsor: Murcian Regional Government Grants; Grant numbers: PSH93/52, 05584/ARQ/07, CTC/DGC/SPH/063/2001, CCE/DGC/IPH/SAR0/1998, CCE/DGC/IPH/SAR/1997, CE/DGC/IPH/SAR/011/1996, CCE/DGC/IPH/SAR/1995, CCE/DGC/IPH/SAR/1994, PSH/93/52.

*Correspondence to: Erik Trinkaus, Department of Anthropology, Washington University, Saint Louis, MO 63130.
E-mail: trinkaus@artsci.wustl.edu

Received 19 May 2010; accepted 23 September 2010

DOI 10.1002/ajpa.21428
Published online 29 November 2010 in Wiley Online Library (wileyonlinelibrary.com).

variable degrees of data on axial and appendicular morphology. The Palomas 92 partial skeleton retains one vertebra, plus humeral, radial, ulnar, femoral, manual and pedal remains, and a partial pelvis. It was discovered partially crushed and heavily cemented in breccia. It has been possible to separate and acid clean many of the bones. Yet, portions of the right elbow, right hand, and left foot remain in blocks of the articulated bones and interstitial matrix, and they cannot be separated without risk of damage to the individual elements. The pelvis is crushed in the breccia, and the pieces are only partially separated from the matrix.

The context

The Sima de las Palomas (37° 47′ 59″ N, 0° 53′ 45″ W) is a natural karstic shaft in the 312 m high Cabezo Gordo hill of Permo-Triassic marble. The shaft was largely emptied of its breccia fill during the 19th century by miners (Supporting Information Fig. S1; Walker, 2001; Walker et al., 2008, 2010), but they left an 18 m deep column of sediment on one side of the karstic shaft. Systematic excavation of its uppermost 3–4 m (the Upper Cutting) has provided abundant Neandertal remains, fauna and lithics. Sampling of the sediment has also been conducted at deeper levels, ~5 m above the foot of the sediment column (the Intermediate Cutting) and to a depth of 5 m beneath the foot of the shaft (the Lower Cutting).

The Upper Cutting (Supporting Information Fig. S2) consists of a largely brecciated massive scree, or éboulis (Conglomerate A), sloping down from the west side, overlain to the east by an infilling of softer, gritting sediment containing angular stone clasts. The two sediment components are separated by a dark-gray horizon, the Upper Gray Layer. The brecciated scree, or éboulis, of Conglomerate A lies on an extensive gray horizon (the Lower Gray Layer). This Lower Gray Layer covers, in turn, another bone-bearing breccia, a heavily cemented cyroclastic fine scree (Conglomerate B) which in turn covers a much looser scree or éboulis. The levels in the Upper Cutting contain abundant Middle Paleolithic lithic and faunal remains and variously complete Neandertal fossils (no diagnostic Upper Paleolithic artifacts or early modern human remains are known from in situ in the Upper Cutting).

A combination of accelerator mass spectrometry (AMS) radiocarbon, laser ablation multicollector plasma mass spectrometry (LA-ICP-MS) uranium-series, optically stimulated luminescence (OSL), and paleoclimatic correlation dating places the remains from above the Upper Gray Layer in the Upper Cutting to ≥40,000 cal years BP (≥35,000 ^{14}C years BP) and those in Conglomerate A to ~50,000–60,000 cal years BP (cf., Walker et al., 2008 and Supporting Information Fig. S3 for dating details). The deeper levels of the sediment column should extend back through much of the Late Pleistocene.

Seven of the isolated Neandertal postcranial elements (Palomas 14, 28, 32, 66, 67, 77, and 86; Supporting Information Table S1) were found in situ in the infilling portion of the Upper Cutting, and therefore they are among the most recent securely dated Neandertals known (Walker et al., 2008). The remainder of the isolated postcrania were discovered ex situ as a result of the miners' work, either on the hillside or deeper within the shaft. They are therefore undated; however several of the elements are partially burned (Palomas 9, 15, 17, and 64), and it appears likely that they derive from one of the gray layers of the Upper Cutting. In any case, all are Late Pleistocene in age and associated with the Middle Paleolithic. These elements include five immature pieces (Palomas 8, 14, 32, 66, and 86), three (Palomas 16, 52, 63) which likely represent small adults but may come from adolescents, and nine mature bones (Palomas 9, 13, 15, 17, 28, 64, 65, 67, and 77).

The Palomas 92 associated postcrania derive from Conglomerate A, between the Upper and Lower Gray Layers. It is therefore older than the seven bones found in situ in the upper infilling, but it may be about the same age as many of the ex situ isolated remains. It represents a young adult of indeterminate sex (see SI).

MORPHOLOGY OF THE PALOMAS POSTCRANIA

The Palomas postcranial sample includes elements which are morphologically diagnostic and/or provide data of paleobiological relevance in a Late Pleistocene context. There are also specimens which provide little more than inventorial mention, since they retain morphological aspects which differ little across Late Pleistocene human samples. The preservation of the bones is described in the Supporting Information, morphometric data are provided for them in Supporting Information Tables S3 to S24, and most of them are illustrated in Supporting Information Figures S4 to S14. Salient aspects of the sample are presented here.

Comparative considerations

The Palomas Neandertal postcrania are assessed using standard morphometrics, discrete traits and cross-sectional geometry as obtainable from the incomplete remains. They are compared principally with MIS 4-3 Neandertals from western Eurasia and to the MIS 3 early modern humans from the same geographical region that followed them closely (Early Upper Paleolithic [EUP] and slightly later (Mid Upper Paleolithic [MUP]) in time. In addition, data as available are included for the southwest Asian Middle Paleolithic modern humans (MPMH) and, to a lesser extent, MIS 5 early Neandertals. Given the dearth of European EUP postcrania (comparative data only from Brassempouy and Mladeč), data are also included from the northwest African Nazlet Khater 2 skeleton. Sites yielding comparative specimens are listed in the Supporting Information.

Comparative data are from personal research, personal communication, and published primary descriptions of the remains. The arm bone comparisons present both the side preserved for Palomas and the pooled right and left sides, given common asymmetry in these features. Other comparisons employ the pooled right and left bones, averaged by individual, as available. The morphometric comparisons consist of boxplots and bivariate plots; in the latter the variables were generally logged (Ln_e) to reduce the scatter among the larger values and/or compare measures with different dimensionalities.

Body size

The Palomas mature postcrania universally give the impression of small body size for Neandertals. Comparisons of available bone length and articular dimensions (see Fig. 1) place them below the Neandertal medians and in several cases below the known Neandertal

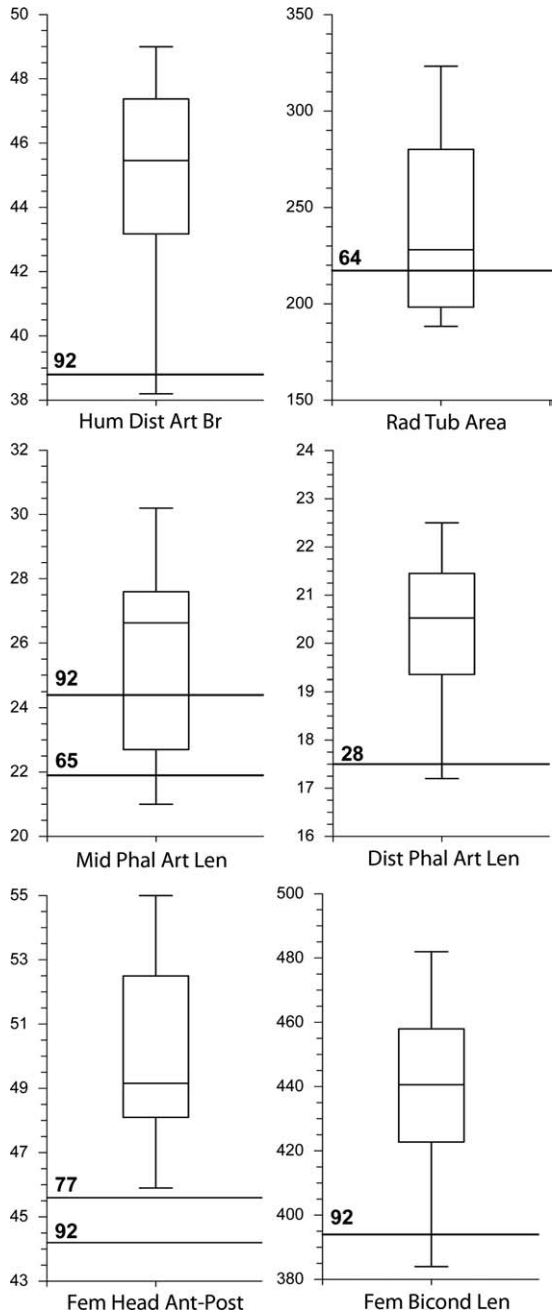

Fig. 1. Box plots of skeletal dimensions for Palomas postcrania specimens compared to distributions of MIS 4-3 Neandertals; Neandertal samples sizes are provided after each measurement. Hum Dist Art Br: humerus distal articular breadth (mm) (21). Rad Tub Area: Radial tuberosity area computed as an ellipse from the tuberosity diameters (mm^2) (11). Mid Phal Art Len and Dist Phal Art Len: manual and distal phalanx 2-4 articular lengths (mm) (31 and 24, respectively). Fem Head Ant-Post: anteroposterior diameter of the femoral head (mm) (11). Fem Bicond Len: femoral bicondylar length (mm) (13).

ranges. Several of these dimensions are for Palomas 92, and hence serve to reflect its overall small body size, but it is joined by the Palomas 28 and 65 manual phalanges, the Palomas 77 femoral head, and to a lesser extent the Palomas 64 radius. Of these comparisons, only the Palomas 92 middle manual phalanx length and the Palomas 64 radial tuberosity area (which combines size and robusticity, but is the only measure available for comparison) are within the interquartile ranges of the Neandertal samples.

The best reflection of body mass, femoral head diameter (Auerbach and Ruff, 2004), is available for Palomas 77 and 92 (45.6 and ~44.2 mm); both are below the MIS 4-3 Neandertal ranges of variation. Even at $+2SE_{est}$ (47.4 mm; see Supporting Information Table S16), the Palomas 92 femoral anteroposterior head diameter is below all but the La Ferrassie 2 female (45.9 mm), which is the lowest plotted value. Among MIS 5-3 Neandertals, only the MIS 5 Krapina 207 and Tabun 1 femora have head diameters as low as the mean estimate for Palomas 92 and the Palomas 77 value. The mean bicondylar femoral length estimate of Palomas 92 (~394 mm) is below the lengths of all European Neandertal femora (the closest is La Ferrassie 2 at 407 mm), it is only above the estimate from the Shanidar 6 femoral diaphysis (~384 mm), and it is approached by the length of the earlier MIS 5 Tabun 1 femur (410 mm). Even at $+2SE_{est}$ (414 mm), it is among the smallest of the European and southwest Asian MIS 5-3 femora.

In addition to these body size indicators, three specimens, the Palomas 63 first rib, the Palomas 16 humeral diaphysis and the Palomas 52 femoral diaphysis (Figs. 3, 5, Supporting Information Figs. S4, S5, and S7), appear morphologically mature in terms of diaphyseal shape, muscle insertion form and (for the diaphyses) percent cortical area (although none of them preserves a metaphysis). Yet, all three are exceptionally small. The Palomas 16 midshaft cortical area of 186 mm^2 is below the range of Neandertal humeri (the closest is the Spy 2 left humerus at 191 mm^2). The Palomas 52 femoral midproximal cortical area (327 mm^2) is well below the Neandertal range; the closest is La Ferrassie 2 at 467 mm^2, and even the small MIS 5 Tabun 1 femur has a cortical area of 484 mm^2.

Body shape

Given the contrast in body shape between the Neandertals and western Eurasian early modern humans, with the former exhibiting elevated body mass to stature proportions compared with the latter (Holliday, 1997a), it is of interest to assess whether the Palomas Neandertals follow the same pattern as the more northern ones. Body proportions can be assessed only for Palomas 92 and only indirectly using femoral proportions. For this assessment, femoral head diameter is assumed to be a reliable proxy for body mass and femoral length reflects stature (Auerbach and Ruff, 2004). Among MIS 4-3 humans, Neandertals, and particularly European Neandertals, have large femoral heads for their femoral lengths (Fig. 2A); the two Neandertals with relatively small femoral heads (Amud 1 and Shanidar 5) are southwest Asian, and the one next to Palomas 92 is the La Ferrassie 2 female. Most of the MUP modern humans and all of the earlier MPMH have relatively smaller femoral heads. Palomas 92 therefore falls among the Neandertals, at the top of the MUP range, but less extreme than most of the European Neandertals. Taking into consideration the estimations of these two dimensions for Palomas 92 (Supporting Information Table S16) would change its position little.

An alternative approach is to compare the femoral diaphyseal rigidity to femoral length of Palomas 92 to other

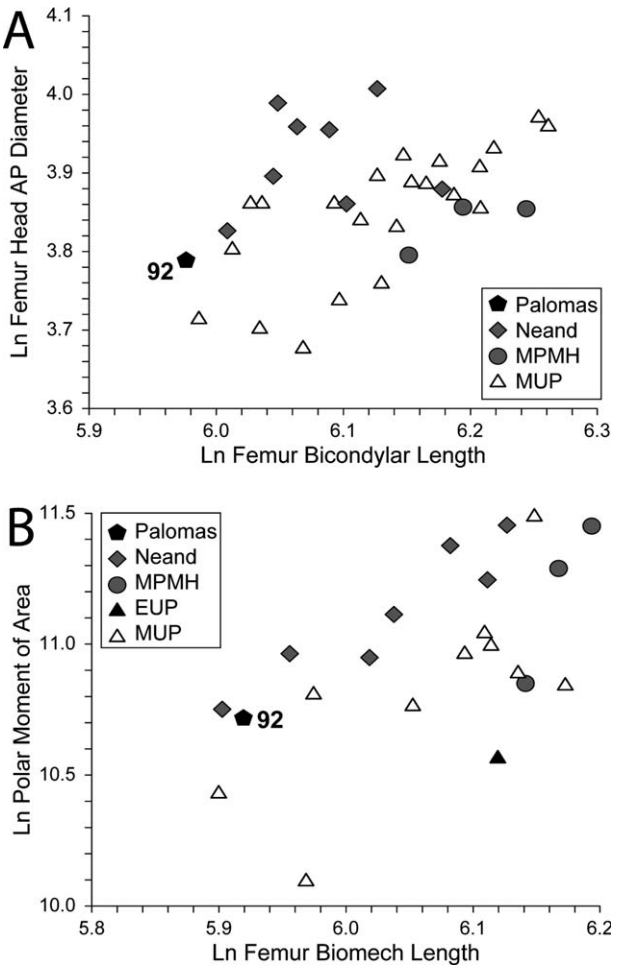

Fig. 2. Ln_e bivariate plots of (**A**) femoral head anteroposterior diameter versus bicondylar length, and (**B**) femoral mid-proximal (65%) polar moment of area versus biomechanical length. MPMH, Middle Paleolithic modern humans; EUP, Early Upper Paleolithic humans; MUP, Mid Upper Paleolithic humans.

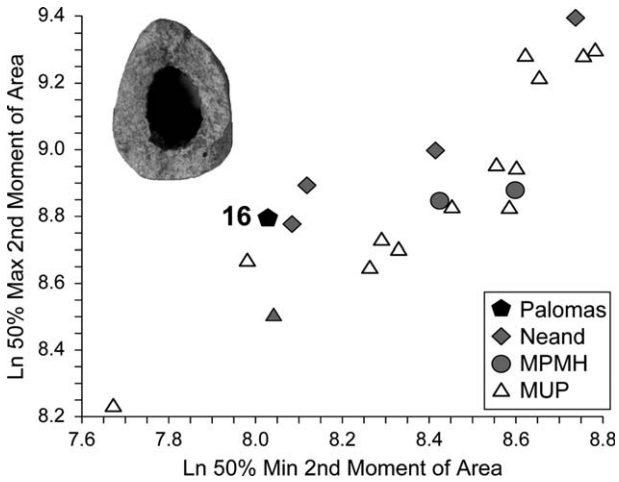

Fig. 3. Ln_e bivariate plot of maximum versus minimum second moments of area for the Palomas 16 humeral midshaft (cross-section provided) versus Late Pleistocene comparative samples. Abbreviations as in Figure 2.

Late Pleistocene remains, assuming that Palomas 92 follows the pattern of little difference in femoral diaphyseal robusticity across these Late Pleistocene femora once they are scaled to estimated body mass times bone length (Trinkaus, 2006a). The plot of mid-proximal (65%) polar moment of area to femoral length (Fig. 2B) largely separates the Neandertals from the early modern humans, a reflection primarily of contrasting body proportions in the context of individual variation in femoral diaphyseal robusticity. Palomas 92 falls along the interface between the Neandertal and MUP samples but close to the Neandertal distribution and above most of the early modern human femora.

These two indirect indicators of body shape for Palomas 92 therefore imply that its body mass relative to stature was close to those of the generally broad Neandertals and above the majority of the western Eurasian more linear early modern humans.

Upper limb postcranial morphology

In the humeral diaphysis Palomas 16 has a relatively narrow, or anterolaterally to posteromedially elongated, diaphyseal cross-section, which is reflected in the comparison of its midshaft maximum and minimum second moments of area to those of other left MIS 4-3 humeri (see Fig. 3). A similar assessment, less precise but with larger comparative sample sizes, is provided by its midshaft index (Table 1). Both comparisons place Palomas 16 close to the Neandertal mean and well above those of the early modern human samples, indicating its substantially less circular humeral midshaft than those of most early modern humans.

The pectoralis major tuberosity of Palomas 16 is at least 7.6 mm wide (Fig. 4 and Supporting Information Fig. S5), which in absolute terms is below the Neandertal range (8.1–12.5 mm) and within the MUP range (2.5–9.1 mm). However, if it is compared to its midshaft circumference (Table 1; a conservative size scaling, since both should reflect musculoskeletal robusticity), the resultant index is within the Neandertal range and matched by only one MUP humerus (Pavlov 1). If the tuberosity was originally broader, on its absent proximal portion, the index would have been above the MUP range.

Although neither of the Palomas 16 nor 92 humeri provides a length for robusticity scaling, it is possible to assess percent cortical areas for them. The Palomas 16 left midshaft is unexceptional in this aspect for a Middle Paleolithic human, and it remains well within the MUP range of variation (Table 1). The Palomas 92 mid-distal diaphysis, however, has a percent cortical area (88.1%) which is at the top of the Late Pleistocene ranges of variation; it is matched only by Regourdou 1 (88.7%), Nahalein-Gev 1 (89.4%) and the earlier Krapina 173 (87.8%).

Neandertals, including the Iberian Oliveira 3 humerus, have been noted to have relatively narrow distal pillars, especially the medial one (Carretero et al., 1997; Trinkaus et al., 2007); a feature variably present among earlier archaic *Homo* (Carretero et al., 2009). The index of the summed pillar thicknesses to olecranon fossa breadth for Palomas 92 (Table 2; Fig. 4 and Supporting Information Fig. S9) is within the range of a variable MUP sample, since it is above the low value for Nahalein-Gev 1 for right humeri and matched by those of Dolní Věstonice 15 and Grotte-des-Enfants 6 in the average values. However, its index is below those of most

TABLE 1. Humeral diaphyseal comparisons for the Palomas Neandertals and comparative MIS 5-3 samples [mean ± SD (N)]

Sample[a]	Humerus left midshaft index[b]	Humerus left pectoralis major index[c]	Humerus left mid-shaft percent cortical area	Humerus right mid-distal percent cortical area
	Palomas 16	Palomas 16	Palomas 16	Palomas 92
Palomas	138.5	≥14.0	76.7	88.1
Neandertals	137.2 ± 7.3 (8)	15.4 ± 1.9 (6)	76.4 ± 2.7 (5)	80.1 ± 4.9 (10)
MPMH	117.1, 123.5, 127.4	–	61.6, 92.1	80.1 ± 6.2 (5)
EUP	114.1	–	83.0	76.6, 81.7
MUP	122.2 ± 9.6 (21)	10.5 ± 2.4 (12)	67.2 ± 7.8 (15)	76.7 ± 8.1 (12)
P-values[d]	0.003	0.002	0.051	0.598

[a] MPMH, Middle Paleolithic modern humans (Qafzeh and Skhul); EUP, Early Upper Paleolithic; MUP, Mid Upper Paleolithic.
[b] Midshaft (maximum/minimum diameters) × 100.
[c] The index from the pectoralis major tuberosity maximum breadth versus the midshaft circumference calculated from the midshaft diameters.
[d] Kruskal-Wallis and Wilcoxon *P*-values across the available comparative samples.

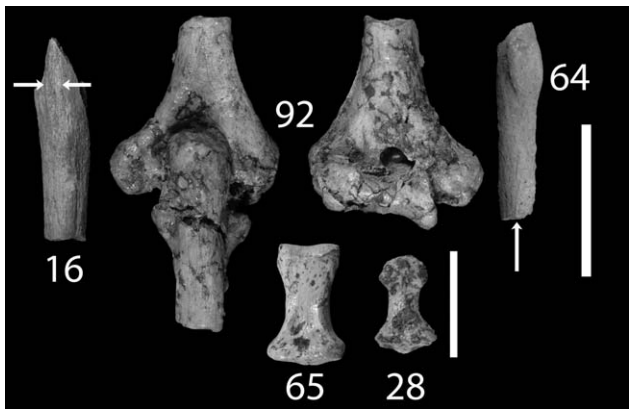

Fig. 4. Upper limb remains from Palomas. Above left to right: Palomas 16 humeral diaphysis in anterior view with the pectoralis major tuberosity indicated; Palomas 92 elbow in posterior view; Palomas 92 distal humerus in anterior view; Palomas 64 radius in medial view with the position of the interosseus crest indicated. Scale bar: 5 cm. Below center: Palomas 65 middle manual phalanx 2-4 and Palomas 28 distal manual phalanx 2-4 in palmar view. Scale bar: 2 cm.

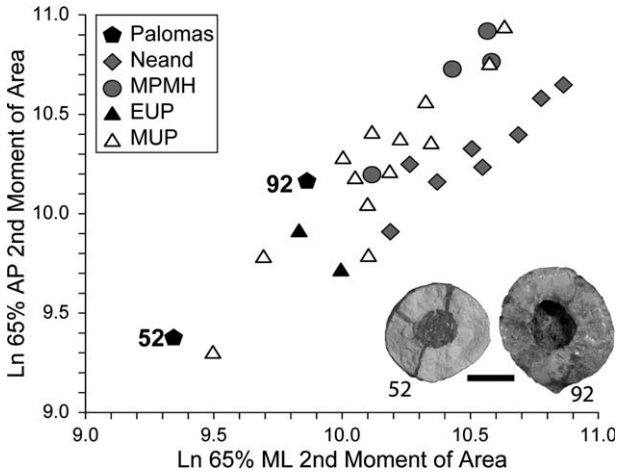

Fig. 5. Ln_e bivariate plot of anteroposterior versus mediolateral second moments of area for the mid-proximal femoral diaphysis (~65%) for Palomas 52 and 92 and Late Pleistocene humans. Sample abbreviations as in Figure 2. Scale bar for cross-sections: 1 cm.

MUP humeri, and it is even below the means of a Neandertal sample, which are significantly lower than those of the MUP (and MPMH) samples. Even for a Neandertal, Palomas 92 has relatively narrow pillars (see Fig. 4).

The Palomas 92 right humerus has a clear septal aperture (Fig. 4 and Supporting Information Fig. S9). In this feature, it joins a number of other MIS 4-3 Neandertals, especially if right and left bones are pooled (Table 2). Although present among MIS 5 MPMH, such apertures are absent from the EUP and MUP samples but common among MIS 5 Neandertals (58%, $N = 12$).

Neandertals proximal ulnae have relatively low coronoid processes (Churchill et al., 1996; Trinkaus, 2006b), which is reflected in the index of coronoid to olecranon height (Table 3). The ranges of variation of the comparative samples are separate, and the Palomas 92 index is moderately high for a Neandertal, within their range of variation, and completely apart from the MPMH and MUP samples. However, the Palomas 64 radial tuberosity is anteromedially positioned relative to the interosseus crest (Table 3; Fig. 4 and Supporting Information Fig. S6; the Palomas 92 radius is insufficiently complete to assess its radial tuberosity orientation). This is the dominant pattern among early modern humans and Neandertal left radii, but it is found in less than half of the Neandertals when right and left values are pooled.

The diagnostic hand remains from Palomas (Fig. 4, Supporting Information Figs. S6, S10, and S11) consist principally of the left trapezium and the proximal and middle phalanges of Palomas 92, plus the Palomas 28 and 65 phalanges. Some additional data are available for the Palomas 15 and 92 metacarpals (MC) and the other three Palomas 92 carpals (Supporting Information Tables S11–S15).

The Palomas 92 left trapezium retains a complete metacarpal 1 facet, one side of an articulation that changes significantly between late archaic and early modern humans, from the dorsopalmarly relatively flat articulations of archaic humans to the more deeply saddle shaped ones of early and recent modern humans (Trinkaus, 1989; Niewoehner, 2001; Marzke et al., 2010). The Palomas 92 trapezium, both in terms of its absolute and relative dorsopalmar curvature subtense (Table 4), is distinct from the Neandertals and shares with the MPMH and MUP individuals the more curved surface of recent humans.

The Palomas 92 trapezium also retains its palmar tubercle, which is gracile for a Neandertal. The comparison

TABLE 2. Humereral distal epiphyseal comparisons for Palomas 92 and comparative MIS 5-3 samples [mean ± SD (N)]

Sample	Humerus right pillar index[a]	Humerus Ave. pillar index[b]	Humerus septal aperture presence[c]
Palomas 92	75.3	75.3	Present
Neandertals	81.5 ± 9.3 (8)	79.0 ± 9.3 (14)	3/11 (7/16)
MPMH	95.2	95.2, 101.2	1/4 (2/5)
EUP	–	–	0/2 (0/2)
MUP	102.7 ± 20.4 (14)	105.6 ± 21.9 (22)	0/15 (0/17)
P-values[d]	0.020	<0.001	0.018 (<0.001)

[a] Humeral ([medial pillar thickness + lateral pillar thickness]/olecranon fossa breadth) × 100.
[b] Same index using right, left or their average as available.
[c] The number with the aperture present, followed by the sample size, is provided for right humeri only and then, in parentheses, for the pooled right and left humeri.
[d] Kruskal-Wallis (pillar indices) and Chi-square (septal apertures) *P*-values across the available comparative samples. All are significant at the $P < 0.05$ level after a sequentially reductive multiple comparison correction.

TABLE 3. Forearm comparisons for the Palomas Neandertals and comparative MIS 5-3 samples [mean ± SD (N)]

	Ulna right coronoid height index[a]	Ulna Ave. coronoid height index[a]	Radial tuberosity anteromedial[b]
Sample	Palomas 92	Palomas 92	Palomas 64
Palomas	124.1	124.1	Anteromedial
Neandertals	118.4 ± 3.9 (7)	118.3 ± 4.4 (10)	5/7 (5/13)
MPMH	134.9	129.9, 124.9, 141.6	1/1 (4/4)
EUP	–	–	1/1 (2/2)
MUP	142.3 ± 8.3 (9)	142.2 ± 8.0 (18)	15/16 (26/28)
K-W *P*-value[c]	0.002	<0.001	0.146 (<0.001)

[a] Ulnar (coronoid height/olecranon height) × 100. Values for right ulnae only, and then followed by values for the pooled (and averaged when both sides are present) right and left ulnae.
[b] The frequencies of anteromedial, as opposed to directly medial, orientation of the radial tuberosity relative to the interosseus crest. Values (# anteromedial/N) are provided for left radii, followed in parentheses by values for pooled right and left radii. The anteromedial categories 1 and 2 of Trinkaus and Churchill (1988) have been pooled together, separate from directly medial (category 3).
[c] Kruskal-Wallis (ulna) and Chi-square (radius) *P*-values across the four comparative samples. All are significant at the $P < 0.05$ level after a sequentially reductive multiple comparison correction, except for the radial tuberosity orientation for left radii.

TABLE 4. Hand comparisons for the Palomas Neandertals and comparative MIS 5-3 samples [mean ± SD (N)]

Sample	Trapezium metacarpal height subtense (mm)[a] Palomas 92	Trapezium metacarpal height index[b] Palomas 92	Trapezium tubercle index[c] Palomas 92	Middle phalanx base breadth index[d] Palomas 65 & 92	Distal phalanx distal breadth index[e] Palomas 28
Palomas	3.7	33.6	28.9	65.8, 54.9	55.4
Neandertals	0.9 ± 0.6 (7)	7.5 ± 4.7 (7)	55.4 ± 8.4 (6)	58.3 ± 4.6 (28)	52.3 ± 6.6 (24)
MPMH	2.3, 4.1	23.0, 31.8	29.4	49.7 ± 4.1 (12)	39.8 ± 3.0 (7)
EUP	–	–	–	50.7, 55.5	40.5
MUP	1.9	16.2	31.3, 33.9, 37.6	49.1 ± 4.0 (25)	41.2 ± 6.8 (19)
K-W *P*-value[f]	0.053	0.053	0.032	<0.001	<0.001

[a] The maximum subtense from the metacarpal articular height chord to the most distally projecting point on the mid metacarpal facet.
[b] The index between the metacarpal height subtense and the articular height of the facet.
[c] The index of the geometric mean of the proximodistal length, the radioulnar thickness, and the dorsopalmar projection of the trapezial tubercle versus the metacarpal facet breadth.
[d] Proximal maximum breadth as a percentage of articular length for middle phalanges 2 to 4. Note that the sample sizes are for phalanges and not for individuals; sample sizes by individual are: Neandertals (12), MPMH (3), EUP (1), MUP (11).
[e] Distal tuberosity breadth as a percentage of articular length for distal phalanges 2 to 4. Note that the sample sizes are for phalanges and not for individuals; sample sizes by individual are: Neandertals (12), MPMH (2), EUP (1), MUP (9).
[f] Kruskal-Wallis *P*-values across the four comparative samples. ANOVA *P*-values for the trapezial comparisons, which take magnitude as well as rank order into account, are 0.014, 0.005, and 0.006 respectively.

of its volume (length × thickness × projection) to its MC1 articular breadth (as an overall size measure) (Table 4) provides an index well below those of other Neandertals and modestly below those of three MUP individuals and of Qafzeh 9.

The Palomas 15 MC2 and especially the Palomas 92 MC4 (Supporting Information Fig. S10) are notable for their thick diaphyseal cortical bone. The approximately midshaft percent cortical areas for them are 80.3% and 94.7%, respectively (Supporting Information Table S13). The Palomas 92 MC5 lacks an opponens digiti minimi crest, a feature that is present in 79.2% ($N = 12$) of the Neandertals. Of more diagnostic importance, the Palomas 65 middle phalanx 2-4 exhibits a relative base

breadth that is at the top of the Neandertal range and completely separate from the early modern humans samples (Table 4). The Palomas 92 middle phalanx 3 has an index which is within the lower portion of the Neandertal range, and it is matched by phalanges of Dolní Věstonice 16, Nazlet Khater 2, and Pataud 6.

The Palomas 28 distal phalanx 2-4 has the rounded distal tuberosity of the Neandertals, lacking ungual spines (Fig. 4 and Supporting Information Fig. S6). The tuberosity is broad relative to phalanx length, despite the tendency of Neandertal distal phalanges to be relatively long (Villemeur, 1994). Its tuberosity breadth to length index places it among the broader of the Neandertal distal phalanges, separate from the early modern humans despite a close value for one of the Sunghir 1 phalanges (Table 4). It is particularly separate metrically and morphologically from the Brassempouy 344 phalanx, despite their proximity in time (Henry-Gambier et al., 2004).

Lower limb postcranial morphology

The Palomas 52 and 92 femora each follows the Neandertal (and archaic *Homo*) pattern of having a subcircular diaphysis with a variably projecting linea aspera but no development of a pilaster (Fig. 5, Supporting Information Figs. S7 and S12). The midshafts of these femora are either eroded (Palomas 52) or distorted (Palomas 92), but it is apparent from their mid-proximal cross-sections (see Fig. 5) and the complete absence of longitudinal sulci adjacent to the linea aspera further distally that they lacked any development of a pilaster.

It is possible to assess their diaphyseal proportions close to the mid-proximal (65% of biomechanical length) diaphyseal position. The Palomas 52 section should be very close to 65%, given the location of the fossilization break at the proximal end of the linea aspera proper. The Palomas 92 section is slightly distal of 65% of its estimated length, at ~62%. Comparison of their anteroposterior (I_x) to mediolateral (I_y) second moments of area (see Fig. 5) places the Palomas 92 femur among the early modern humans and distinct from the Neandertals. The Palomas 52 femur also appears to be among the early modern humans, even though $I_x < I_y$; this position is partly a result of the convergence of the Neandertal and early modern human slopes for small femora.

It is difficult to assess the robusticity of the Palomas femora, since it would require an approximation of body mass for them (Ruff et al., 1993). However, even though the Palomas 92 femoral head diameter and mid-proximal rigidity were employed above in the assessment of body shape, it is possible to combine them with length to approximate the bone's diaphyseal robusticity (Fig. 6A). The resultant plot, in which femur length (for beam length) times head diameter (as linearly correlated with body mass) provides a baseline (cf., Ruff et al., 1993; Auerbach and Ruff, 2004), places Palomas 92 with the more robust of the MIS 4-3 femora despite the small comparative sample size. A comparison of gluteal tuberosity breadth to femur length provides a similar pattern, in which Palomas 92 is relatively robust (Fig. 6B). Incorporating femoral head diameter as a proxy for body mass to scale gluteal tuberosity size provides a similar pattern but greatly reduces comparative sample sizes. The Palomar 92 femur therefore exhibits a level of crural robusticity at least similar to those of other Neandertals.

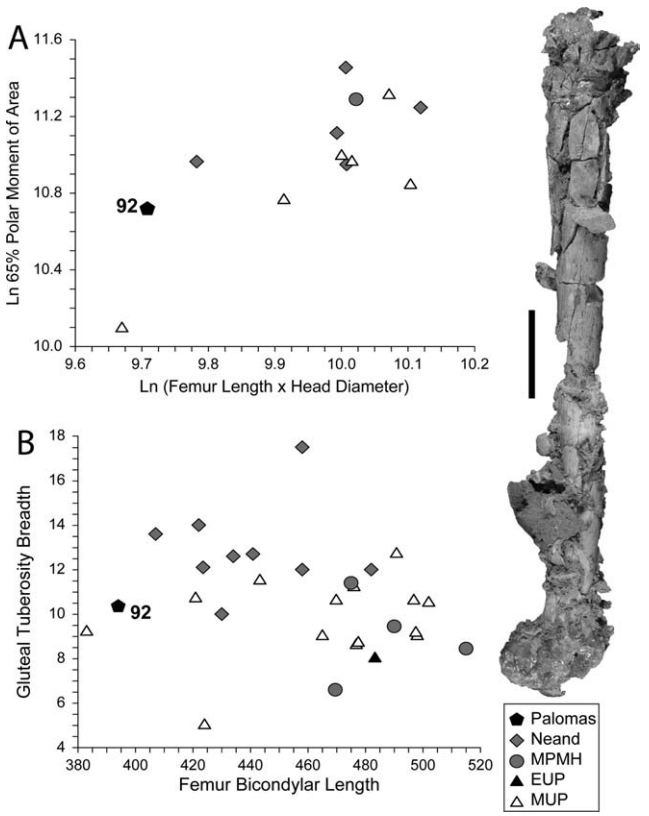

Fig. 6. Bivariate plots of **A**: $\ln_e$ mid-proximal polar moment of area versus femoral length times head diameter, and (**B**) gluteal tuberosity breadth versus femoral length for Palomas 92 and comparative Late Pleistocene samples. Sample abbreviations as in Figure 2. Scale bar for the lateral view of the right femur: 5 cm.

There is little of note in the Palomas 92 tarsals and metatarsals; their overall morphology and especially the pattern of metatarsal torsion indicate the full formation of pedal arches with a fully adducted hallux (despite the fossilization distortion of the tarsometatarsal articulations (Fig. 7 and Supporting Information Fig. S13). The one aspect of note concerns the robusticity of the middle proximal phalangeal diaphyses (Fig. 8 and Supporting Information Fig. S14), which tends to be elevated in Middle Paleolithic (archaic and modern) humans relative to those of earlier Upper Paleolithic humans, in the context of similar levels of femoral and tibial robusticity (Trinkaus, 2005; Trinkaus and Shang, 2008). In a plot of the polar moments of area computed from the external diaphyseal diameters versus articular lengths (see Fig. 8), there is minimal overlap between the Middle Paleolithic and MUP phalanges. The two phalanges from Palomas 92 fall within the very small overlap zone between these Middle versus Upper Paleolithic clusters.

DISCUSSION

Affinities

It is apparent from these considerations that the Palomas human postcrania conform to the morphological pattern of the Neandertals, most of which is shared with archaic *Homo* generally (Trinkaus, 2006c). In an MIS 4-3 context of the northwestern Old World, the distinctive

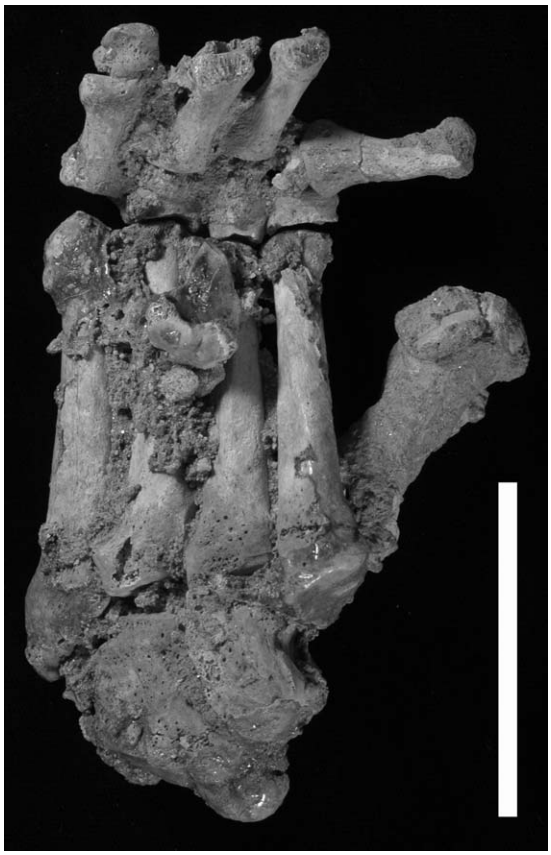

Fig. 7. Dorsal view of the Palomas 92 left foot, with the three primary blocks (tarsals and lateral metatarsals, first metatarsal, metatarsal heads and phalanges) in approximate in situ positions. Scale bar: 5 cm.

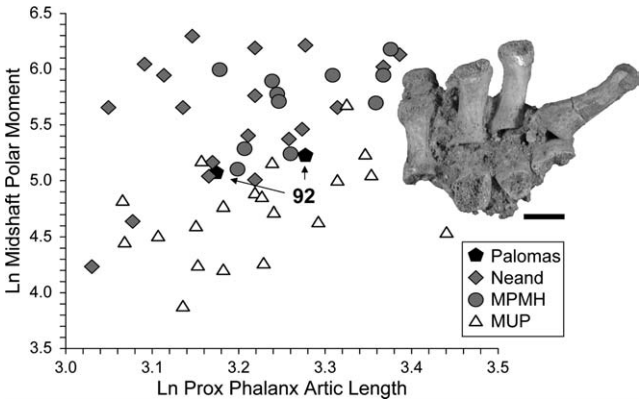

Fig. 8. Bivariate plot of the external midshaft polar moment of area (from the diaphyseal diameters) versus articular length for the proximal pedal phalanges 2-4. Right and left phalanges, when available for a digit, were averaged, but there are between 1 and 3 data points per individual depending on the number of phalanges preserved. Numbers of individuals are: Neandertals, 9; MPMH, 4; MUP, 8. Dorsal view of the proximal pedal phalanges is provided; scale bar: 1 cm.

features include the ovoid humeral midshaft and pectoralis major breadth of Palomas 16, the thin humeral pillars of Palomas 92, the ulnar coronoid height of Palomas 92, the manual middle phalangeal epiphyseal breadth of Palomas 65 (and to a lesser extent that of Palomas 92), the distal phalanx tuberosity form and breadth of Palomas 28, and the femoral diaphyseal cross-sectional discrete morphology of Palomas 52 and 92. In addition, the inferred body proportions of Palomas 92, based on its incomplete femora, place it largely with the Neandertals but principally separate from the Middle Paleolithic modern humans.

The two morphological features which separate the Palomas postcrania from the Neandertals are the cross-sectional proportions of the Palomas 92 mid-proximal femur with its greater anteroposterior dimensions, and the more sellar MC1 facet of its trapezium. A similar femoral diaphyseal shape is evident in the Middle Pleistocene Castel del Guido femur (Mallegni et al., 1983) but not in the Late Pleistocene one from Santa Croce (Trinkaus, pers. observ.). The trapezial MC1 articulation is the first instance of this derived modern human morphology in an archaic specimen. Palomas 92 also has a relatively gracile trapezial tubercle and hand phalanges.

As previously noted (Walker et al., 2008), the Palomas 28 distal phalanx derives from the Upper Cutting infilling and hence is among the most recent Neandertals known, dating to a time period during which there were early modern humans in at least southeastern Europe (Trinkaus et al., 2003) and Aurignacian assemblages (probably indicating early modern humans) in the Pyrenees (Zilhão, 2006). Palomas 92 is older, similar in age to many European Neandertals, and the remainder of the Palomas postcrania are undiagnostic or are undated within the Late Pleistocene but may well derive from the earlier MIS 3 gray layers. In any case, these postcrania join the Palomas cranial, mandibular and dental remains (Walker et al., 1998, 2008, 2010) in confirming the presence of Neandertals in southeastern Spain through at least through MIS 3 up until ~40,000 cal BP.

Postcranial robusticity

The Palomas postcrania exhibit variable degrees of the postcranial robusticity that characterizes the Neandertals and, at least in the lower limb, early modern humans (Trinkaus, 2000). In the upper limb, this is reflected in the Palomas 16 humeral diaphyseal shape and pectoralis major tuberosity, the percent cortical areas of the Palomas 92 mid-distal humerus and of the Palomas 15 and 92 metacarpal diaphyses, and the middle and distal phalanges of Palomas 65 and 28. In the lower limb, the Palomas 92 femur appears, despite estimation, to be among the more robust of the Late Pleistocene femora in diaphyseal rigidity and gluteal tuberosity size.

Yet, the trapezial tubercle, the manual middle phalanx breadths, and the pedal proximal phalangeal robusticity of Palomas 92 place it among the more gracile of the Neandertals. The first two may represent individual variation. It is unlikely that the latter implies anything about its levels of foot protection (cf., Trinkaus, 2005), given its morphometric position adjacent to both Middle Paleolithic and MUP distributions.

Body shape

None of these Palomas remains provides a direct indication of body breadth or distal-proximal limb segment proportions. However, the assessments of femoral relative head diameter and diaphyseal robusticity suggest that at least Palomas 92 was close to the more northern

European Neandertals in having "arctic" body proportions (cf., Holliday, 1997b). At least with respect to relative head diameter, it contrasts with two of the three southwest Asian Neandertals (Amud 1 and Shanidar 5) in this indirect body shape reflection. Given the more southern location, and more temperate MIS 3 climate (Carrión et al., 2003), of the Sima de las Palomas, this pattern raises the issue of ecogeographical body shape variation among the Neandertals.

Body size

At the same time, one feature that appears to distinguish the Palomas Neandertal postcranial remains from those of most other MIS 4-3 Neandertals is their overall diminutive dimensions. This is partly influenced by the small size of the Palomas 92 individual, and its influence on several of the morphometric measurements employed, but it is also evident in the Palomas 28, 64, 65, and 77 isolated remains, two of which (28 and 77) derive from the Upper Cutting infilling. If the Palomas 16 and 52 diaphyseal sections are included as mature specimens, as is suggested by their external morphologies and cortical thicknesses, the small size of the sample is further emphasized.

It is possible that the small size of these Neandertals is merely a sampling bias, in terms of sampling a relatively small population and/or almost exclusively females. Body size sexual dimorphism among the Neandertals appears to have been close to that evident among recent humans (Trinkaus, 1980), but a combination of sampling bias in both parameters might explain the small dimensions of these individuals.

Yet, it is also tempting to see this small size as reflecting ecogeographical body size variation within Neandertals, given the more southern location and especially the temperate early last glacial climate of southeastern Iberia (Barron et al., 2003; Carrión et al., 2003). In this scenario, the small size of the Palomas individuals would be a reflection of Bergmann's Rule, in which body mass varies inversely with environmental temperature across widely dispersed species. There are moderately robust patterns conforming to Bergmann's Rule across endothermic vertebrates (Mayr, 1963) and recent human populations (Ruff, 1994), even though it has been difficult to establish a distinct thermoregulatory physiological benefit for larger body mass (or the related surface area to body mass ratio) in cold stressed samples of extant humans (Steegmann, 2007).

As a preliminary assessment of this issue, despite the small sample sizes available, one can use a latitudinal boundary of 40° N latitude to separate more "northern" from more "southern" Neandertals. This latitude separates Neandertals from Mediterranean Europe (Italy and Iberia south of the Pyrenees) and southwest Asia from the more northern remains from Europe. The only other European MIS 4-3 postcranial specimens south of this line providing meaningful dimensions are the Oliveira 3 and 4 fragmentary humerus and tibia (Trinkaus et al., 2007), the incomplete Zafarraya 1 femur (García Sanchez, 1986), and the Santa Croce (Bisceglie) 1 femur diaphysis (Cardini, 1955). Given preservation and available data of these remains, size comparisons are limited. However, it is possible to assess roughly their overall dimensions relative to more northern Neandertals.

The Oliveira 3 olecranon fossa breadth (29.5 mm) is unexceptional for a Neandertal, falling within one standard error of the European Neandertal mean (29.9 ± 2.0, $N = 12$), and the Oliveira 4 midshaft cortical area (369 mm^2) is between the La Ferrassie 2 female (297 mm^2) and four male European Neandertals (436.0 ± 7.6 mm^2).

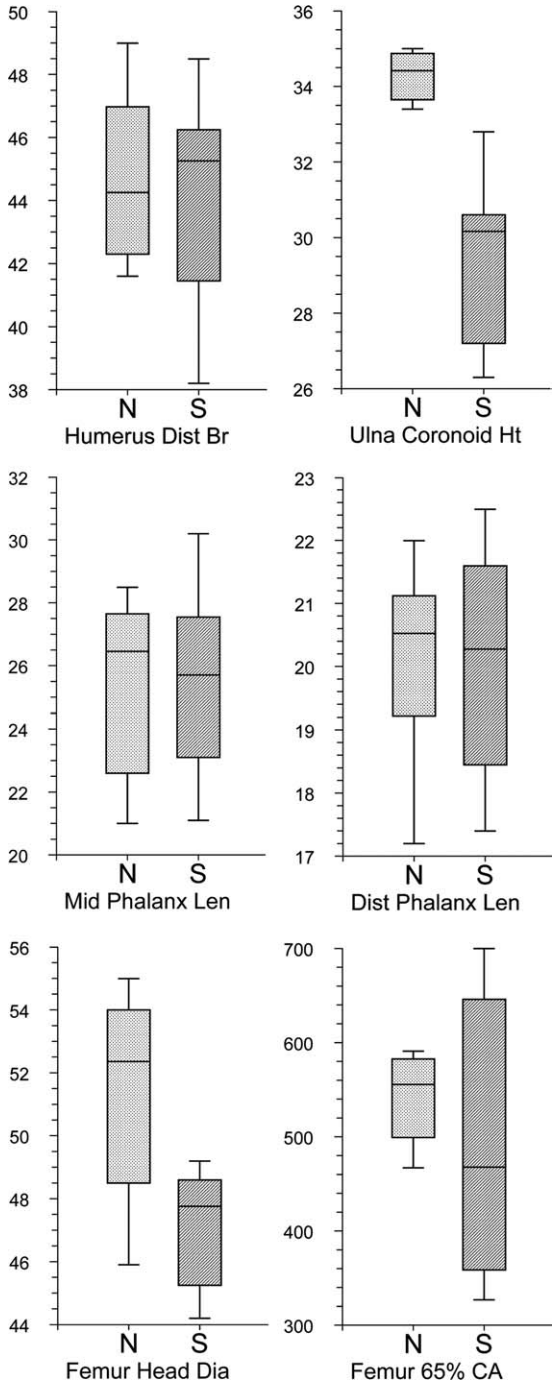

Fig. 9. Comparisons of "northern" (N) versus "southern" (S) Neandertal appendicular dimensions, for humeral distal articular breadth ($P = 0.841$), ulnar coronoid height ($P = 0.011$), middle and distal manual phalanx 2-4 articular lengths ($P = 0.726$ and 0.957), femur anteroposterior head diameter ($P = 0.027$), and femur mid-proximal (65%) cortical area ($P = 0.337$). Samples are separated at the 40° N latitude. In millimeters except for the cortical area, which is in mm^2. Wilcoxon P-values for the individual "northern"/"southern" comparisons are provided after each one above.

The Zafarraya 1 femur subtrochanteric diaphyseal "total area" (computed from the external diameters using an ellipse formula) of 748 mm^2 is modestly below a European Neandertal mean (775.4 ± 63.5 mm^2, $N = 7$). The Santa Croce 1 femur has a smaller subtrochanteric "total area" (617 mm^2), and its midshaft "total area" (667 mm^2) is below the mean of a variable more northern European Neandertal sample (702.2 ± 72.0 mm^2, $N = 9$). The available postcranial dimensions of the El Sidrón Neandertals, north of the 40° N latitude [although included by Rosas et al. (2006) in their southern sample], are relatively large, with the one complete femoral head (El Sidrón 1609) having a diameter that is among the largest known for the European Neandertals and three humeri having olecranon fossa breadths that are at or slightly below the Neandertal mean (Rosas, pers. comm.). There is therefore only a suggestion, combining the Palomas, other southern Iberian postcrania and one Italian specimen, for generally smaller dimensions among these "more temperate" Neandertals.

If the Palomas data are combined with the other principal sample of more southern Neandertals, those from the southwest Asian sites of Amud, Kebara, and Shanidar, any pattern becomes less clear (see Fig. 9). In femoral head diameter these more southern Neandertals are distinctly smaller than their more northern European counterparts, with a modest overlap of the ranges of variation and a significant difference between the distributions; the difference is not a sex bias, since at least Amud 1, Kebara 2, and Shanidar 4 are pelvically sexed as male. In the less directly relevant but comparable ulnar coronoid height, the difference is more pronounced. However, in distal humeral articular breadth, manual phalanx lengths, and femoral mid-proximal cortical area, there are no differences between the two samples.

CONCLUSION

The isolated postcranial remains from the Sima de las Palomas plus the associated postcrania of Palomas 92 provide a substantial but fragmentary sample of Neandertal axial and appendicular remains from Mediterranean Europe. The sample consists almost entirely of small individuals, at or below the lower size limits of the known European Neandertals, but the sample largely conforms to the patterns of postcranial morphology documented elsewhere for these late archaic humans (the exceptions being the trapezial MC1 facet and the femoral diaphyseal proportions of Palomas 92). These aspects include humeral diaphyseal shape, distal humeral configuration, proximal ulnar form, manual phalangeal breadths, femoral diaphyseal shape, and probable body proportions. They also exhibit variable appendicular robusticity. Although many of these features may be shared with archaic *Homo* generally, they contrast with those of Middle and Upper Paleolithic early modern humans. Moreover, there is little to indicate a difference between the Palomas postcrania and those of more northern Neandertals other than body size and a more anteroposteriorly expanded femoral diaphysis.

ACKNOWLEDGMENTS

Cabezo Gordo's landowners and the Cabezo Gordo S.A. quarry are thanked for permitting excavation at Sima de las Palomas. The field research has received support from the mayor and town council of Torre Pacheco and the Earthwatch Institute (1994–2001). A. Rosas kindly provided data on the El Sidrón postcrania.

LITERATURE CITED

Arsuaga JL, Villaverde V, Quam R, Martínez I, Carretero JM, Lorenzo C, Gracia A. 2007. New Neandertal remains from Cova Negra (Valencia. Spain). J Hum Evol 52:31–58.

Auerbach BM, Ruff CB. 2004. Human body mass estimation: a comparison of "morphometric" and "mechanical" methods. Am J Phys Anthropol 125:331–342.

Barron E, van Andel TH, Pollard D. 2003. Glacial environments. II. Reconstructing the climate of Europe in the last glaciation. In: van Andel TH, Davies W, editors. Neanderthals and modern humans in the European landscape during the last glaciation. Cambridge, UK: McDonald Institute for Archaeological Research. p 57–78.

Barroso-Ruíz C, Lumley MA de, Caparrós M, Verdú L. 2003. Los restos humanos Neandertalenses de la cueva del Boquete de Zafarraya. In: Barroso-Ruiz C, editor. El pleistocene superior del la cueva del Boquete de Zafarraya. Seville: Consejería de Cultura de la Junta de Andalucía. p 327–387.

Cardini L. 1955. Giacimento musteriano della Grotta Santa Croce in Bisceglie e scoperta di un femora unamo neandertaliano. Quaternaria 2:312.

Carretero JM, Arsuaga JL, Lorenzo C. 1997. Clavicles, scapulae and humeri from the Sima de los Huesos site (Sierra de Atapuerca, Spain). J Hum Evol 33:357–408.

Carretero JM, Haile-Selassie Y, Rodriguez L, Arsuaga JL. 2009. A partial distal humerus from the Middle Pleistocene deposits at Bodo, Middle Awash, Ethiopia. Anthropol Sci 117:19–31.

Carrión JS, Yll EI, Walker MJ, Legaz AJ, Chaín C, López A. 2003. Glacial refugia of temperate. Mediterranean and Ibero-North African flora in south-eastern Spain: new evidence from cave pollen at two Neanderthal man sites. Global Ecol Biogeogr 12:119–129.

Churchill SE, Pearson OM, Grine FE, Trinkaus E, Holliday TW. 1996. Morphological affinities of the proximal ulna from Klasies River Mouth main site: archaic or modern? J Hum Evol 31:213–237.

Fabre V, Condemi S, Degioanni A. 2009. Genetic evidence of geographical groups among Neanderthals. PLoS ONE 4:e5151.

García Sánchez M. 1986. Estudio preliminar de los restos Neandertalenses del Boquete de Zafarraya (Alcaucín, Málaga). In: Pellicer M, editor. Homenaje a Luis Siret (1934-1984). Seville: Consejería de Cultura de la Junta de Andalucía.5:49–56.

Giacobini G, Lumley MA de. 1988. Les fossiles humains de la Caverna delle Fate (Finale, Ligurie italienne) et la définition des caractères néandertaliens au début du Würm. Etud Rech Archéol Univ Liège 30:53–66.

Hambücken A. 1997. La variabilité géographique des Néandertaliens: apport de l'étude du membre supérieur. Anthropol Préhist 108:109–120.

Henry-Gambier D, Maureille B, White R. 2004. Vestiges humains des niveaux de l'Aurignacien ancien du site de Brassempouy (Landes). Bull Mém Soc Anthropol Paris 16:49–87.

Holliday TW. 1997a. Body proportions in Late Pleistocene Europe and modern human origins. J Hum Evol 32:423–447.

Holliday TW. 1997b. Postcranial evidence of cold adaptation in European Neandertals. Am J Phys Anthropol 104:245–258.

Mallegni F, Mariani-Costantini R, Fornaciari G, Longo ET, Giacobini G, Radmilli AM. 1983. New European fossil hominid material from an Acheulian site near Rome (Castel del Guido). Am J Phys Anthropol 62:263–274.

Marzke MW, Tocheri MW, Steinberg B, Femiani JD, Reece SP, Linscheid RL, Orr CM, Marzke RF. 2010. Comparative 3D quantitative analyses of trapeziometacarpal joint surface curvatures among living catarrhines and fossil hominins. Am J Phys Anthropol 141:38–51.

Mayr E. 1963. Animal species and evolution. Cambridge MA: Belknap.
Niewoehner WA. 2001. Behavioral inferences from the Skhul/Qafzeh early modern human hand remains. Proc Natl Acad Sci USA 98:2979–2984.
Rosas A, Martínez-Maza C, Bastir M, García-Tabernero A, Lalueza-Fox C, Huguet R, Ortiz JE, Julià R, Soler V, de Torres T, Martínez E, Cañaveras JC, Sánchez-Moral S, Cuezva S, Lario J, Santamaría D, de la Rasilla M, Fortea J. 2006. Paleobiology and comparative morphology of a late Neandertal sample from El Sidrón. Asturias, Spain. Proc Natl Acad Sci USA 103:19266–19271.
Ruff CB. 1994. Morphological adaptation to climate in modern and fossil hominids. Yrbk Phys Anthropol 37:65–107.
Ruff CB, Trinkaus E, Walker A, Larsen CS. 1993. Postcranial robusticity in *Homo*. I. Temporal trends and mechanical interpretations. Am J Phys Anthropol 91:21–53.
Steegmann AT Jr. 2007. Human cold adaptation: an unfinished agenda. Am J Hum Biol 19:218–227.
Trinkaus E. 1980. Sexual differences in Neanderthal limb bones. J Hum Evol 9:377–397.
Trinkaus E. 1989. Olduvai Hominid 7 trapezial metacarpal 1 articular morphology: contrasts with recent humans. Am J Phys Anthropol 80:411–416.
Trinkaus E. 2000. The "Robusticity Transition" revisited. In: Stringer C, Barton RNE, Finlayson C, editors. Neanderthals on the edge. Oxford: Oxbow Books. p 227–236.
Trinkaus E. 2005. Anatomical evidence for the antiquity of human footwear use. J Archaeol Sci 32:1515–1526.
Trinkaus E. 2006a. The lower limb remains. In: Trinkaus E, Svoboda JA, editors. Early modern human evolution in Central Europe: the people of Dolní Věstonice and Pavlov. New York: Oxford University Press. p 380–418.
Trinkaus E. 2006b. The upper limb remains. In: Trinkaus E,Svoboda JA, editors. Early modern human evolution in Central Europe: the people of Dolní Věstonice and Pavlov. New York: Oxford University Press. p 327–372.
Trinkaus E. 2006c. Modern human versus Neandertal evolutionary distinctiveness. Curr Anthropol 47:597–620.
Trinkaus E, Churchill SE. 1988. Neandertal radial tuberosity orientation. Am J Phys Anthropol 75:15–21.
Trinkaus E, Moldovan O, Milota Ş, Bîlgar A, Sarcină L, Athreya S, Bailey SE, Rodrigo R, Gherase M, Higham T, Bronk Ramsey C, van der Plicht J. 2003. An early modern human from the Peştera cu Oase. Romania. Proc Natl Acad Sci USA 100:11231–11236.
Trinkaus E, Maki J, Zilhão J. 2007. Middle Paleolithic human remains from the Gruta da Oliveira (Torres Novas). Portugal. Am J Phys Anthropol 134:263–273.
Trinkaus E, Shang H. 2008. Anatomical evidence for the antiquity of human footwear: Tianyuan and Sunghir. J Archaeol Sci 35:1928–1933.
Villemeur I. 1994. La Main des Néandertaliens. Paris: CNRS.
Walker MJ. 2001. Excavations at Cueva Negra del Estrecho del Rio Quípar and Sima de las Palomas del Cabezo Gordo: two sites in Murcia (south-east Spain) with Neanderthal skeletal remains, Mousterian assemblages and late Middle to early Upper Pleistocene fauna. In: Milliken S, Cook J, editors. A very remote period indeed. Oxford: Oxbow Books. p 153–159.
Walker MJ, Gibert J, Sánchez F, Lombardi AV, Serrano I, Eastham A, Ribot F, Arribas A, Cuenca A, Sánchez JA, García J, Gibert L, Albadalejo S, Andreu JA. 1998. Two SE Spanish Middle Palaeolithic sites with Neanderthal remains: Sima de la Palomas del Cabezo Gordo and Cueva Negra del Estrecho del Rio Quípar (Murcia Province). Internet Archaeol 5. Available at: http://intarch.ac.uk/journal/issue5/walker.
Walker MJ, Gibert J, López MV, Lombardi AV, Pérez-Pérez A, Zapata J, Ortega J, Higham T, Pike A, Schwenninger JL, Zilhão J, Trinkaus E. 2008. Late Neandertals in southeastern Iberia: Sima de las Palomas del Cabezo Gordo. Murcia, Spain. Proc Natl Acad Sci USA 105:20631–20636.
Walker MJ, Lombardi AV, Zapata J, Trinkaus E. 2010. Neandertal mandibles from the Sima de la Palomas del Cabezo Gordo. Murcia, southeastern Spain. Am J Phys Anthropol 142:261–272.
Zilhão J. 2006. Chronostratigraphy of the Middle-to-Upper Paleolithic transition in the Iberian peninsula. Pyrenae 37:7–84.

Neandertal Postcranial Remains from the Sima de las Palomas del Cabezo Gordo, Murcia, Southeastern Spain: Supporting Information

Michael J. Walker, Jon Ortega, Mariano V. López and Erik Trinkaus

I. STRATIGRAPHIC PROFILES OF THE SIMA DE LAS PALOMAS

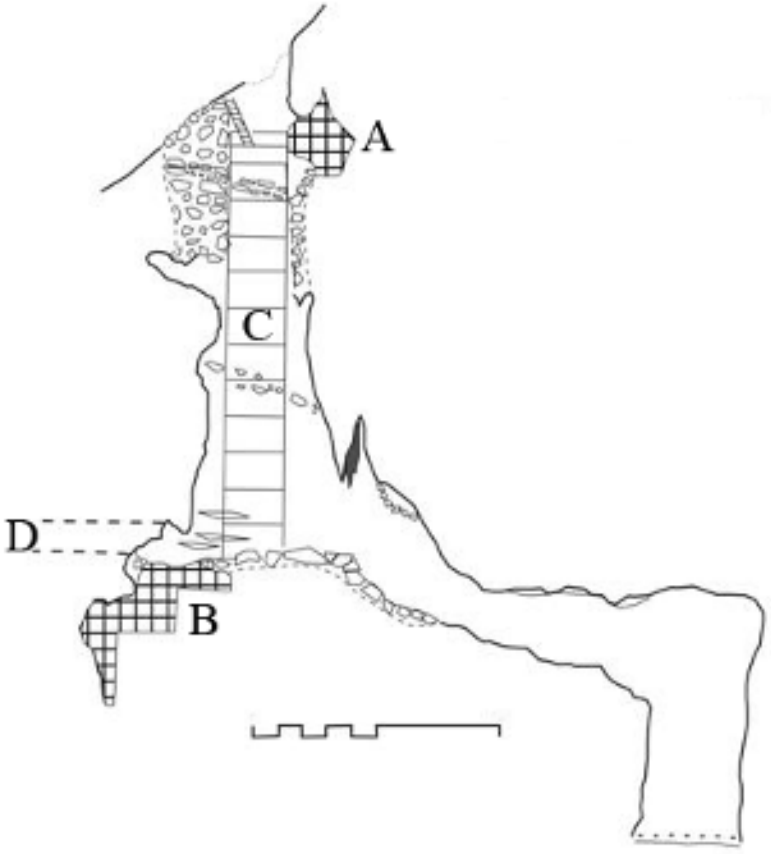

Figure S1. Vertical diagram of the main chamber and breccia column of the Sima de las Palomas, indicating the areas of excavation to date. A: Upper Cutting excavation area; B: Lower Cutting excavation area; C: scaffolding; D: tunnel extended from the lower portion to the outside by 19th century miners. Scale = 10 m.

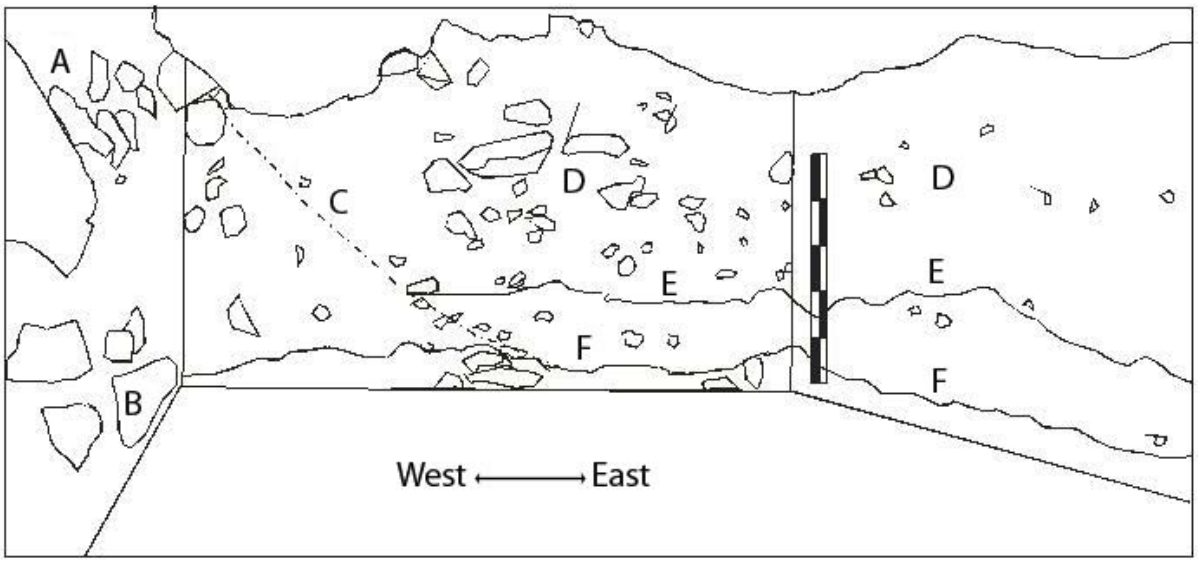

Figure S2. Stratigraphic rendition of the 2008 Upper Cutting profiles. A: Éboulis above the northwestern corner of the excavated cutting; B: Levels 2m-2o breccia below the Upper Gray Layer and containing human bones; C: Projection of the scree slope (éboulis) onto the rear profile; D: Infilling of the Upper Cutting above the scree slope and the gray levels; E: Uppermost limit (levels ~2h-2i) of lens of gray sediment mainly in the northeastern area of the cutting; F: Lower limit of gray ashy sediment (levels 2m-2o) in the northern and eastern area of the cutting. Scale = 1 m.

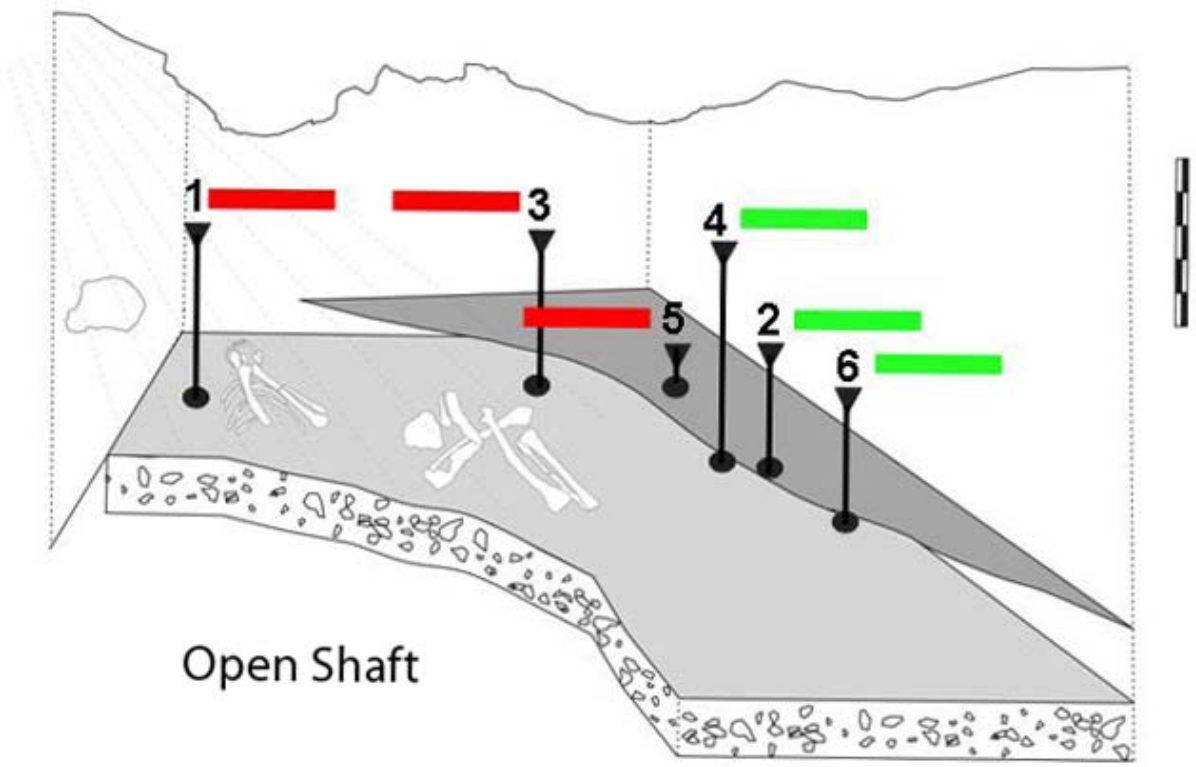

Figure S3. Schematic rendering of the Upper Cutting with the vertical and horizontal positions of the dated samples. The Upper and Lower Gray Layers are in dark and light gray respectively. The red-tagged samples are from the upper éboulis (Conglomerate A), and the green-tagged samples are from the upper infilling. The black triangles indicate the positions of the samples, and the black circle below each one indicates its position on the excavation horizontal grid. Note that the scree slope between the upper éboulis and the infilling of the Upper Cutting slopes from upper left to lower right across the left (west) side of the Upper Cutting (see Fig. S2), such that the stratigraphic positions of the dated samples change across the excavated area. Calibration of the radiocarbon dates was done using CalPal quickcal2007 ver.1.5 (www.calpal.de). For dating details, see Walker et al. (2008). Errors are given as 1 sigma.

1: Palomas 92 metacarpal (Spit 2h) – from three LA-ICP-MS Uranium series estimates (54,100 ± 3,850 cal BP)
2: Unburnt bone (Spit 2i) – LA-ICP-MS Uranium series (43,800 ± 750 cal BP)
3: Unburnt bone U-series (51,000 ± 1,250 cal BP)
4: Burnt bone cemented to the Palomas 59 mandible – radiocarbon (39,691 ± 926 cal BP (34,450 ± 600 ^{14}C BP))
5: Burnt sediment (Spits 2k-2l) – OSL (54,700 ± 4,700 cal BP)
6: Burnt rabbit bones (Spit 2i-2l) – radiocarbon (40,070 ± 849 cal BP (35,030 ± 270 ^{14}C BP))

II. PRESERVATION AND AGES-AT-DEATH OF THE ISOLATED PALOMAS POSTCRANIA

The isolated postcranial remains from the Sima de las Palomas are all fragmentary. Some of them are clearly immature based on the presence of unfused epiphyses. Others are mature (late adolescent or adult) based on preserved and fully fused epiphyses and/or general size and morphology. There are several, however, such as the Palomas 63 rib 1, the Palomas 16 humeral diaphysis and the Palomas 52 femoral diaphysis, which do not preserve age diagnostic epiphyseal regions, appear generally mature in their morphology, but are unusually small for an adult Neandertal. They are considered as possibly immature.

Table S1. Inventory of the isolated human postcranial remains from the Sima de las Palomas (SP).

SP#	Identification	Maturity	Provenience	Discovery Date
8	Axis (cervical vertebra 2)	immature	Hillside rubble	1993
9	Axis (cervical vertebra 2)	mature	Hillside rubble	1993
13	Fibula diaphysis left	mature	Hillside rubble	1994
14	Ulna proximal left	immature	Upper Cutting level 2b	9 July 1994
15	Metacarpal 2 diaphysis and head right	mature	Main chamber rubble	1994
16	Humerus diaphysis left	immature or small?	Hillside rubble (?)	1994
17	Humerus trochlea and epicondyle left	mature	Hillside rubble	1994
28	Manual distal phalanx 2-4	mature	Upper Cutting level 2g	6 July 1995
32	Humerus proximal diaphysis and epiphysis right	immature	Upper Cutting level 2i	10 July 1995
52	Femur diaphysis left	immature or small?	Hillside rubble	2 August 1997
63	Rib 1 right	immature or small?	Hillside rubble	23 July 1999
64	Radius diaphysis left	mature	Hillside rubble	23 July 1999
65	Manual middle phalanx 2-4	mature	Shaft scaffolding tower	9 August 1999
66	Proximal pedal phalanx 2-5	immature	Upper Cutting level 2k	31 July 2000
67	Pedal middle phalanx	mature	Upper Cutting level IA	29 July 2001
77	Femur head	mature	Upper Cutting level 2b	28 July 2003
86	Pedal proximal phalanx 2-5	immature	Upper Cutting level 2g	23 July 2004

Palomas Isolated Axial Remains

Palomas 8: Axis (C2) – Immature

The centrum and the articular facets without the tip of the odontoid process. Maximum preserved breadth: 38.7 mm; maximum preserved height: 21.4 mm.

The immature status is based on its absence of the caudal annular ring and of the tip of the odontoid process. Given that 1) the facets/pedicles fuse to the sides of the odontoid process by 3-4 years post-natal, 2) those portions fuse to the centrum by 4-6 years post-natal, and 3) the tip of the odontoid process fuses to its base by ~12 years post-natal (Scheuer and Black, 2000), the age-at-death of the specimen is best seen as between 6 and 12 years post-natal.

Palomas 9: Axis (C2) – Mature

The bone retains the odontoid process, the cranial left articular facet, the left body and the abraded caudal body. The maximum preserved height is 30.3 mm.

Figure S4. Dorsal views of the Palomas 8 and 9 axis (C2) vertebrae (left), cranial view of the Palomas 92 T12 vertebra (center), and cranial view of the Palomas 63 right rib 1. Scale bar: 5 cm.

Palomas 63 : Rib 1 Right – Immature or Small Adult

The bone preserves the neck and tubercle and the shaft ventrally to close to the costal cartilage surface. It is small and therefore represents an immature individual or a small adult. It

has hard matrix encrustations on its surface, cranially and especially caudally. Maximum preserved length: 51.8 mm.

Palomas Isolated Upper Limb Remains

Palomas 16: Humerus Left – Mature?

Humeral diaphysis from midshaft (very close to the distal end of the deltoid tuberosity) to the middle of the pectoralis major tuberosity. Maximum preserved length is 68.2 mm.

The bone is possibly immature, based on its small size. However, given increases in percent cortical area of the humerus through adolescence (Ruff, 2010), the midshaft percent cortical area (76.7) essentially on the Neandertal adult mean (76.4 ± 2.7, N = 5; see Table 1) implies that it is mature or near mature (late adolescent). It is considered in the comparisons as a small adult, bearing in mind that it might represent an adolescent.

Palomas 17: Humerus Left – Mature

The bone retains only the medial trochlea and the anterior medial epicondyle, which had been burned. Maximum mediolateral dimension is 32.5 mm.

Figure S5. Views of the Palomas isolated humeral remains. Left: Palomas 16 left humerus in anterior (left) and lateral (right) views). Right: Palomas 32 immature proximal right humerus in anterior (above) and posterior (below) views. Below middle: Palomas 17 distal left humerus in anterior view. Scale bar: 5 cm.

Palomas 32: Humerus Right – Immature

The bone consists of a complete proximal metaphysis with the surgical neck and the complete head and tubercle epiphysis cemented onto the metaphysis. The maximum preserved length is 46.0 mm, and its maximum breadth is 32.2 mm.

Given that the epiphysis is completely unfused and that it normally fuses during the middle to late adolescent years (Scheuer and Black, 2000), this suggests a late juvenile or early adolescent age for this specimen.

Palomas 14: Ulna Left – Immature

The proximal end of a very immature left ulna, crushed in laterally. Maximum preserved length is 36.5 mm; maximum anteroposterior dimension is 19.8 mm.

Palomas 64: Radius Left – Mature

The bone preserves the proximal diaphysis and the tuberosity. The distal break is largely transverse at the proximal end of the interosseus crest. The proximal break is oblique anteromedioproximal to posterolaterodistal at the proximal end of the tuberosity. The tuberosity is complete. The surface of the bone is slightly powdery, and there is a hard but thin layer of mineral matrix on the external surface. Maximum preserved length is 67.3 mm.

Figure S6. Isolated antebrachial and manual remains from Palomas. Left: Palomas 64 left proximal radial diaphysis in anterior (A), distal (D) and medial (M) views. Center: Palomas 15 right metacarpal 2 distal diaphysis and head in palmar (P) and radial (R) views. Above right: Palomas 65 manual middle phalanx 2-4 in dorsal (D) and palmar (P) views. Below right: Palomas 28 manual distal phalanx 2-4 in dorsal (D) and palmar (P) views. Scale bar: 5 cm.

Palomas 15: Metacarpal 2 Right – Mature

The complete head and distal half of the diaphysis of a second metacarpal. Digit number and side determined by the oblique slope to the distal left head, hence the radial side of a metacarpal 2 head. Maximum preserved length is 39.0 mm.

Palomas 65: Manual Middle Phalanx 2-4 – Mature

Complete bone with slight dorsal base abrasion. Maximum length is 23.1 mm.

Palomas 28: Manual Distal Phalanx 2-4 – Mature

Complete bone with trivial rounding of the tuberosity (which may have slightly reduced its tuberosity breadth). Maximum length is 19.5 mm.

Palomas Isolated Lower Limb Remains

Palomas 77: Femur Head – Mature

A largely complete femoral head without any of its articular margins. There is a small area of surface bone on the exposed distal trabeculae 9.5 x 5.8 mm which, on the basis of the fovea capitis orientation, should be inferior neck. Side is indeterminate. The trabeculae show no signs of an epiphyseal surface or fusion line, so it is considered to be fully mature. The maximum diameter, which is approximately the anteroposterior diameter, is 45.6 mm.

Palomas 52: Femur Diaphysis Left – Immature or Small Adult

Two pieces of femoral diaphysis which fit cleanly together. The external surface is slightly eroded but intact, and the medullary cavity is filled with hard matrix. The proximal end has the proximal spreading of the muscle lines from the linea aspera, the beginning of the spiral line, and the distal portion of the gluteal buttress. The proximal break is distal of the lesser trochanter. The irregular distal break, based on linea aspera morphology and general contour, should be close to midshaft. The break in the middle of the piece, near the linea aspera proximal spread, should be close to the 65% cross-section. The clean break at ~65% permits photographic cross-sectional analysis; the irregular distal break does not allow such transcription. Maximum preserved length is 100.8 mm.

The bone could be adolescent or mature. Based on size, it is either an unusually small adult or an immature individual. Based on morphological estimates of the positions of the 65% and 80% cross-sections using cross-sectional morphology and especially posterior muscle markings, the distance between them is ~50 mm. That estimate provides a biomechanical length (proximal neck to average of the distal condyles) of ~333 mm, or basically 300-350 mm. This range is below any of the Neandertal adult femoral biomechanical lengths (the closest are Shanidar 6 (~366 mm), La Ferrassie 2 (386 mm) and the MIS 5 Tabun 1 (391 mm). Among early modern humans, it is matched by the very small Minatogawa 2 to 4 femora (332, 353 and 334 mm), and approached by Nahal ein Gev 1 (365 mm). In addition, the well-marked muscle lines are similar to those of an adult, and the small medullary cavity [or high percent cortical area: 84.7 (Table S16), which is essentially on an adult Neandertal mean of 84.4 ± 5.9, N = 8] (Figure S7) indicates mature or late adolescent status (Ruff et al., 1994; Ruff, 2010).

The preserved landmarks are insufficient for a reliable length estimation for any scaling.

Palomas 13: Fibula Left – Mature

Diaphyseal section from distal of the neck to approximately midshaft. Maximum preserved length is 80.7 mm.

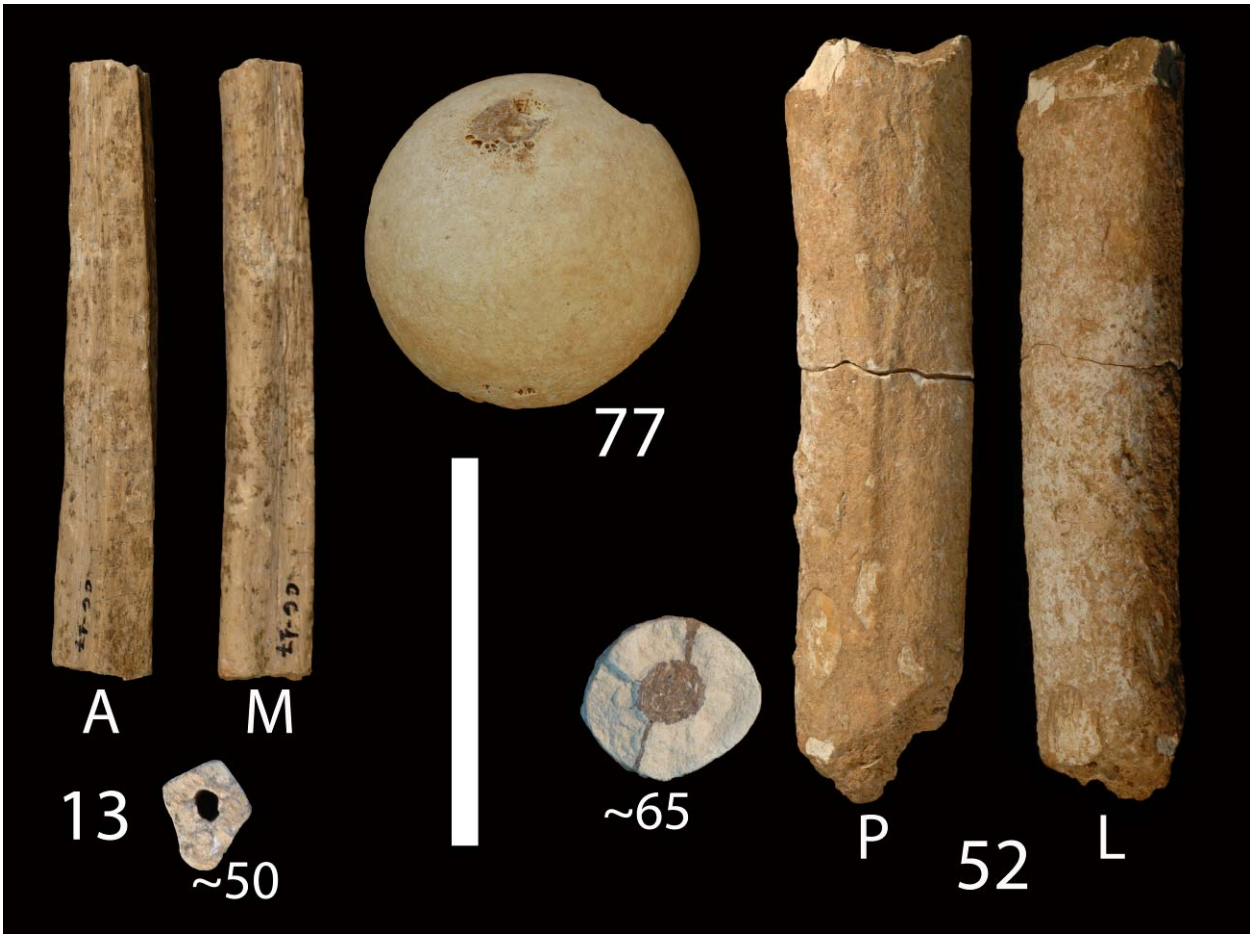

Figure S7. Isolated lower limb remains from Palomas. Left: Palomas 13 left proximal fibular diaphyseal section in anterior (A) and medial (M) views, plus the approximately midshaft cross-section. Center: articular view of the Palomas 77 isolated femoral head. Right: posterior (P) and lateral (L) views of the Palomas 52 proximal femoral diaphysis, plus its approximately 65% (mid-proximal; ~65%) cross-section. Scale bar: 5 cm.

Palomas 66: Pedal Proximal Phalanx 2-5 – Immature

Complete bone without any trace of the proximal epiphysis. The clear waisting of the diaphysis relative to the articular/metaphyseal ends makes it unlikely to be manual (Pyle et al., 1971). Maximum length is 15.0 mm.

Palomas 86: Pedal Proximal Phalanx 2-5 – Immature

Complete immature bone without the proximal epiphysis, heavily encrusted in carbonate matrix. Closely resembles Palomas 66. Maximum length is 14.4 mm.

Palomas 67: Pedal Middle Phalanx 2-4 Left? – Mature

Complete bone with a thin layer of encrustation over the full surface. Given that the distal facet slopes to the left in dorsal view, assuming that the distal interphalangeal articulation would orient laterally, the bone becomes a left phalanx. The size and clear diaphysis separated from the epiphyses makes it unlikely that it is a fifth digit phalanx. Maximum length is 15.5 mm.

III. PRESERVATION OF THE PALOMAS 92 ASSOCIATED PARTIAL POSTCRANIUM

Table S2. Inventory of the Palomas 92 postcrania. As noted below, the right elbow remains, the left anterior tarsal to pedal phalanx bones, and the left metacarpal and manual phalanx remains each forms a cemented block of bones, which cannot be cleaned or separated further without damage to the bones. All of the bones except Palomas 92oo are from Upper Cutting level 2h; Palomas 92oo is from the 2h/2k interface.

SP#	Identification	Discovery Date	Field #
92a	Cuboid left	31 July 2005	SP05H004
92b	Lateral cuneiform left	31 July 2005	SP05H004
92c	Metatarsal 1 left	31 July 2005	SP05H004/008
92d	Metatarsal 2 left	31 July 2005	SP05H004/005/011
92e	Metatarsal 3 left	31 July 2005	SP05H004/005
92f	Metatarsal 4 left	31 July 2005	SP05H004/005
92g	Metatarsal 5 left	31 July 2005	SP05H004
92h	Pedal proximal phalanx 2 left	31 July 2005	SP05H005
92i	Pedal proximal phalanx 3 left	31 July 2005	SP05H005
92j	Pedal proximal phalanx 4 left	31 July 2005	SP05H005
92k	Pedal proximal phalanx 5 left	31 July 2005	SP05H005
92l	Pedal middle phalanx 2-4 left	31 July 2005	SP05H007
92m	Pedal middle phalanx 2-4 left	31 July 2005	SP05H007
92n	Pedal middle phalanx 5 left	31 July 2005	SP05H005
92o	Lateral hallucal sesamoid left	31 July 2005	SP05H011
92p	Medial hallucal sesamoid left	31 July 2005	SP05H004
92q	Metacarpal 3 left	31 July 2005	SP05H009
92r	Metacarpal 4 left	31 July 2005	SP05H009/104
92s	Metacarpal 5 left	31 July 2005	SP05H009
92t	Manual proximal phalanx 3 left	31 July 2005	SP05H009
92u	Manual proximal phalanx 4 left	31 July 2005	SP05H009
92v	Manual proximal phalanx 5 left	31 July 2005	SP05H009

SP#	Identification	Discovery Date	Field #
92w	Manual middle phalanx 3 left	31 July 2005	SP05H009
92x	Manual middle phalanx 4 left	31 July 2005	SP05H009
92y	Manual distal phalanx 3 left	31 July 2005	SP05H009
92z	Metacarpal 2 head right	1 August 2005	SP05H013
92aa	Trapezium left	4 August 2005	SP05H100
92bb	Trapezoid left	4 August 2005	SP05H100
92cc	Metacarpal proximal epiphysis	1 August 2005	SP05H020
92dd	Metacarpal proximal epiphysis and diaphysis	1 August 2005	SP05H021/SP05H032
92ee	Metacarpal head	4 August 2005	SP05H104
92ff	Humerus distal right	1 August 2005	SP05H016
92gg	Ulna proximal right	1 August 2005	SP05H016
92hh	Ulna distal right	1 August 2005	SP05H016
92ii	Radius proximal right	1 August 2005	SP05H016
92jj	Triquetral left	1 August 2005	SP05H016
92kk	Pisiform left?	1 August 2005	SP05H016
92ll	T12 thoracic verterbra	1 August 2005	SP05H036
92mm	Femur proximal diaphysis and trochanters right	29 July, 4 Aug 2005	SP05H002/071B
92nn	Femur distal diaphysis with lateral condyle right	1 August 2005	SP05H014
92oo	Femur trochanters to mid-distal diaphysis left	4, 7 August 2005	SP05H071A/107
92pp	Fibula distal diaphysis left	9 August 2004	--
92qq	Ilium fragment	31 July 2005	SP05H010
92rr	Ilium fragment	1 August 2005	SP05H040
92ss	Ilium fragments and sacrum	4 August 2005	SP05H085

The identified bones of this individual are numbered (SP 92a to 92z, SP 92aa to 92ss) in the approximate order in which they were found in the field, keeping associated elements (foot bones, hand bones, femora) together. They are organized here in anatomical order: axial, arm, hand, leg and foot. All indications are that it is a fully mature individual; the only other age indicator is the degree of fusion of the ventral sacral bodies. Sex is currently indeterminate; it is a very small individual, but there is no population reference for it for body size.

Axial Remains

Palomas 92ll: Thoracic Vertebra (T12)

The body is largely complete. The annular rings are present and fused on to the centrum for 12 mm around the dorsal half of the caudal body, especially on the right side. There are also traces of the annular rings on the cranial body adjacent to the spinal canal. Remaining edges are eroded. The neural arches are largely complete, as are the articular facets and the spinous process. The lateral transverse processes are damaged. The spinal canal retains matrix, and a fragment of bone is cemented to the caudal body. The dorsal end of the spinous process is eroded. All of the primary portions of the vertebra are fused. The maximum preserved dorsoventral diameter is 58.9 mm, and maximum preserved transverse diameter is 41.6 mm on the broken transverse processes.

The cranial facets are fully coronal in orientation, but the caudal facets are more sagittally oriented. This suggests that it is a T-12.

Figure S8. Ventral view of the Palomas 92 sacrum, crushed in matrix against portions of the right and left ilia. Scale bar: 5 cm.

Palomas 92ss: Sacrum

The ventral surface of the extremaly fragile sacrum is exposed in a block of breccia, with the ventral bodies of the S1 to the S3 exposed, especially on the right side. The right pelvic sacral foramen is fully evident, but the other foramina are absent or buried in breccia. The S1-S2 and S2-S3 ventral body fusion lines are readily apparent, and there is a clean separation between the S3 body and the absent S4 body. The promontory has been eroded, as have the lateral margins.

Arm Bones Right (distal humerus, proximal ulna, proximal radius) right

The elbow bones are cemented together, having been acid extracted from a breccia block. They cannot be separated without individual bone damage. The pieces are in anatomical connection, but there are cracks with minor distortion in all three bones. All of the epiphyses are fused, indicating a fully mature individual. There are no apparent pathological lesions.

Palomas 92ff: Humerus Right – Distal

The bone retains the complete distal epiphysis and the diaphysis up to the proximal supracondylar crests. The proximal break is transverse and even. The epicondyles are complete. The anterior capitulum has been pushed proximally. The lateral trochlea is in small pieces. However, the breadths of the distal end (olecranon fossa, distal articular and epicondylar) should be accurate or minimally altered. Maximum proximodistal length, from the distal trochlea to the diaphyseal break, is 64.0 mm.

Palomas 92gg: Ulna Right – Proximal

The proximal ulna consists of two pieces, separated by 3–6 mm, cemented onto the distal humerus. The proximal piece consists of the olecranon with 26 mm of the dorsal surface; it is intact, but the articular surface is obscured. The distal piece has the complete coronoid process and radial facet plus ~34 mm of the proximal shaft distal of the coronoid process. The radius is cemented onto the radial facet and the proximolateral diaphysis.

Palomas 92hh: Ulna Right – Distal

The complete head and part of the distal diaphysis of the right ulna. The styloid process is absent, but it may be a piece of bone adherent to the dorsolateral head. There is no trace of the pronator quadratus tuberosity. Maximum preserved length is 30.7 mm.

Palomas 92ii: Radius Right – Proximal

The bone retains the head, neck and the dorsal corner of the tuberosity. It is fused on to the humerus and ulna as though it were in full pronation, with the tuberosity pointing posterolaterally. There is an oblique crack across the neck, but it is glued with little (≤1 mm) separation. The distal break is oblique. Maximum preserved length on the medial side is 30.2 mm.

Figure S9. Anterior (A), posterior (P), medial (M) and lateral (L) views of the Palomas 92 right elbow, with the distal humerus and the proximal radius and ulna cemented in articulation. Scale bar: 5 cm.

Hand Bone Right

Palomas 92z: Metacarpal 2 Right

The head and the distal diaphysis with abrasion to the radial head. Maximum preserved length is 25.1 mm.

Hand Bones Left

These hand bones consist of two proximal carpals, two distal carpals, the distal portions of the three ulnar metacarpals, the three ulnar proximal phalanges, the middle phalanges 3 and 4, and the distal phalanx 3. All of them except the carpals bones were discovered cemented together in a block of breccia. It has been possible, through acid cleaning, to expose most of the surfaces, but the thin layers of carbonate that cemented the bones together cannot be removed without damage to the bones. The carpal bones were found separately in breccia.

Palomas 92jj: Triquetral Left

Complete bone with abrasion to the ulnar side. Maximum length is 11.5 mm.

Palomas 92kk: Pisiform Left?

Partial bone with most of the facet side absent, and therefore principally the palmar side is preserved. It is insufficient to determine its projection (or dorsopalmar thickness). The

maximum preserved (not original) dimensions are 11.1 and 6.8 mm respectively for the length and thickness. The side is based on association with the left triquetral.

Palomas 92aa: Trapezium Left

A complete bone with minor edge abrasion to the radial metacarpal 1 facet and the edges of the scaphoid and trapezoid facets. There is breccia remaining wihin the palmar sulcus adjacent to the tubercle. There is an irregularity on the dorsal ulnar metacarpal 1 facet, which is from fossilization erosion. Maximum radioulnar breadth is 20.1 mm.

Palomas 92bb: Trapezoid Left

A complete bone with minor edge abrasion and calcite adherent to the metacarpal 2 facet. Maximum dorsopalmar dimension is 9.6 mm.

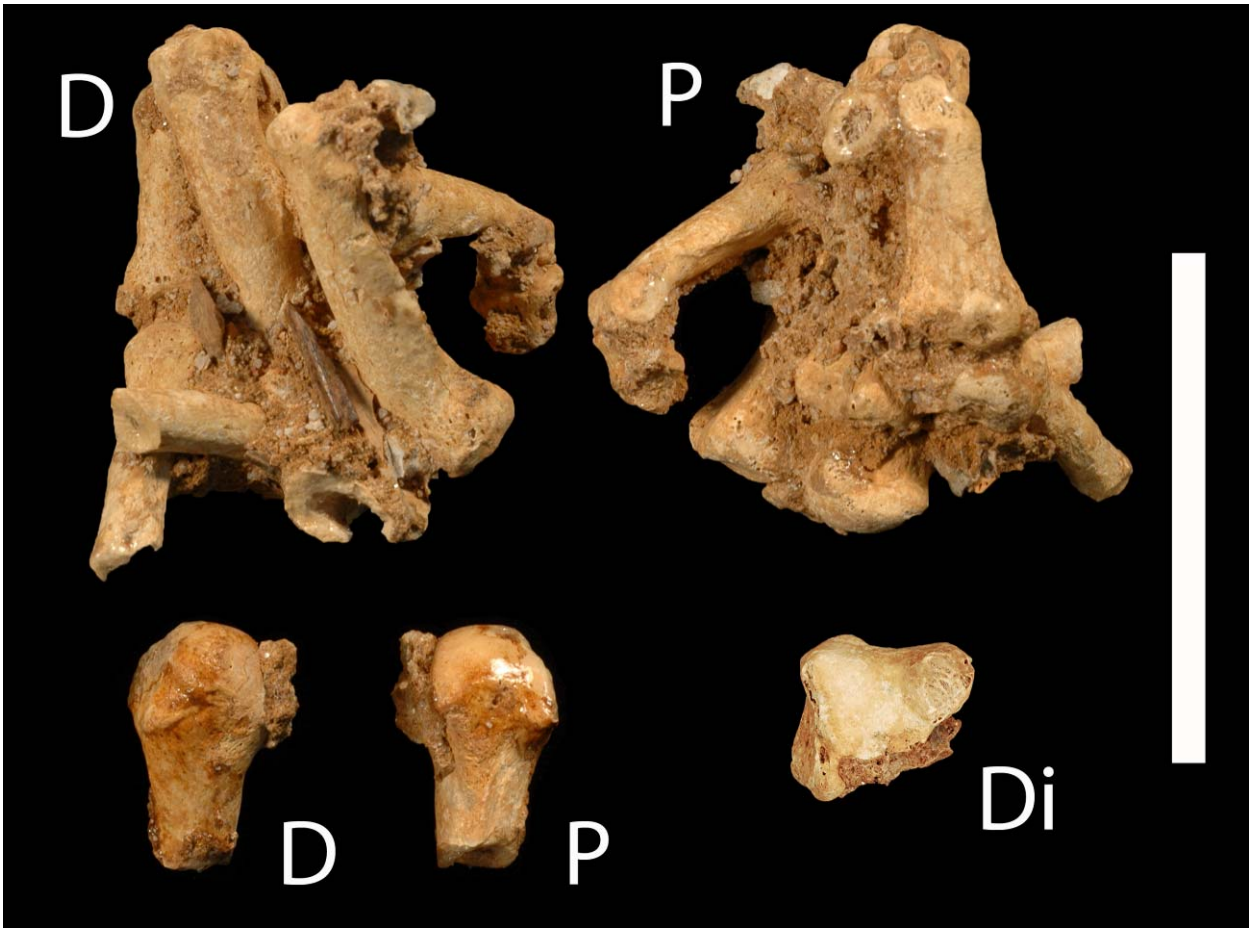

Figure S10. Above: approximately dorsal (D) and palmar (P) views of the Palomas 92 cemented left metacarpals and manual phalanges. Below left: dorsal (P) and palmar (P) views of the right distal metacarpal 2. Below right: distal view (Di) of the left trapezium; the irregularity on the ulnar metacarpal 1 facet is from postmortem erosion. Scale bar: 5 cm.

Palomas 92q: Metacarpal 3 Left

A section of the probably dorsal distal diaphysis and beginning of the flare for the head. Cemented between the metacarpal 4 head and the proximal phalanx 3 base. Maximum preserved length is 18.2 mm; maximum preserved breadth is 9.9 mm.

Palomas 92r: Metacarpal 4 Left

A complete head and the distal approximately two-thirds of the diaphysis. Cemented between the metacarpal 3, the proximal phalanx 3 and 4 bases, and the metacarpal 5 shaft. Maximum preserved length is 33.6 mm; maximum preserved breadth (head) is 11.5 mm.

Palomar 92s: Metacarpal 5 Left

The head missing the palmar surface plus about two-thirds of the diaphysis. The bone is cemented between matrix, the metacarpal 4, and the proximal phalanges 4 and 5. Maximum preserved length is 34.4 mm.

Palomas 92t: Proximal Manual Phalanx 3 Left

Complete bone, with the based cemented to the proximal phalanx 4 and the metacarpals 3 and 4, and the distopalmar shaft cemented to the middle phalanx 3 and matrix. Maximum preserved length is 41.0 mm.

Palomas 92u: Proximal Manual Phalanx 4 Left

Complete bone with the base partly buried in the adjacent metacarpal heads and proximal phalangeal bases. The palmar shaft is below matrix, the metacarpal 4 and the middle phalanx 4. Maximum preserved length is 39.0 mm.

Figure S11. Radial view of the Palomas 92 third ray manual phalanges (left) and approximately dorsal views of the proximal manual phalanges 3 to 5 (right). Scale bar: 5 cm.

Palomas 92v: Proximal Manual Phalanx 5 Left

The base and shaft, cemented to the metacarpal 5, the proximal phalanx 4 and the middle phalanx 4. Maximum preserved length is 27.4 mm.

Palomas 92w: Middle Manual Phalanx 3 Left

Complete bone, cemented to the proximal and distal phalanges 3. Maximum preserved length is 25.6 mm.

Palomas 92x: Middle Manual Phalanx 4 Left

The base, cemented to the proximal phalanges 4 and 5. Maximum preserved length is 8.4 mm.

Palomas 92y: Distal Manual Phalanx 3 Left

The base, cemented to the middle phalanx 3. Maximum preserved length is 9.0 mm.

Lower Limb Remains

The preserved pelvic remains consist of fragments of the ilia preserved in breccia, either alone (92qq and 92rr) or in the same block as the ventral sacrum (92ss). They provide little information.

The right and left femora of Palomas 92 (based on size and morphology) derive from several blocks of breccia. They are broken, cracked and distorted. Yet, three sections of the right femur fit together reasonably well with variably eroded breaks, permitting assessment of overall length. All of the preserved epiphyses (the trochanteric ones plus the right lateral condyle) are fully fused, indicating a mature age.

Palomas 92mm: Femur Right – Proximal Diaphysis and Trochanters

This piece consists of two pieces that fit cleanly together, despite minor erosion along their transverse proximal diaphyseal join. They are described separately but are now one piece. Their combined length is 217.5 mm.

The more distal section (SP05H002) consists of a short section of mid-proximal diaphysis, with the full cross-section exposed about the 60-65% position, then ~28 mm of the full circumference distal of the transverse end. Further distally, there is ~30 mm of the anterolateral diaphysis continuing to an eroded distal end. Maximum preserved length is 62.1 mm.

The more proximal piece (SP05H071B) is a badly crushed and twisted section of the trochanters and proximal diaphysis. The distal 18-19 mm of the diaphysis is intact with the full contour, and it fits well with SP05H002. The diaphysis is then compressed mediolaterally up to the lesser trochanter but with little length distortion. The spiral line and the gluteal tuberosity are evident for most of their lengths, but on twisted pieces. The greater trochanter is anteroposteriorly crushed and then twisted, such that its mediolateral direction is now anteroposterior, with the medial side anterior with respect to the mid-proximal diaphysis. The anterior surface, digital fossa and superior surface of the greater trochanter are largely present, but they are broken and distorted. Maximum preserved length is 159.5 mm.

Palomas 92nn: Femur Right – Midshaft to Distal Epiphysis

The distal femoral diaphysis and epiphysis from near or just proximal of midshaft to the condyles, with most of the lateral condyle preserved. The midshaft is compressed anteromedial to posterolateral. The popliteal area is intact posteriorly, cracked laterally, and compressed and covered in matrix anteriorly and medially. The medial condyle retains only a small 12 mm wide by 33.5 mm long section of its lateral (intercondylar) articular surface. The lateral condyle is largely intact with abrasion to the lateral edge of the articular condyle and to a strip along the rim of the condyle laterally. The lateral epicondyle is intact. The lateral patellar surface is present under matrix, and its preserved anterolateral edge is very close to the original margin. The sequence of pieces from the near midshaft break to the distal end is tightly fitting, with one crack having a 1 mm expansion. Maximum preserved length is 185 mm.

Palomas 92oo: Femur Left – Trochanters to Distal Diaphysis

The left femur consists of two pieces, one proximal (SP05H107) and the other midshaft to distal diaphysis (SP05H071A) that join cleanly ~70% of biomechanical length. They are described separately, but their combined preserved length is 245.0 mm.

The more distal piece (SP05H071A) starts proximally with a clean break across the mid-proximal diaphysis (near 70%), just proximal of the juncture of the spiral line and the linea aspera. It then, going distally, has 23-24 mm of intact diaphyseal cross-section. Distally, it is then anteroposteriorly compressed to the supracondylar region. There is little length distortion, except for what might be related to the twisting of the individual pieces. The most distal edge of the piece is posterolateral. Based on bone curvature and surface smoothness, plus comparisons to the more complete right femur, the distal extent should be close to the popliteal surface. Maximum preserved length is 185.0 mm.

The smaller proximal piece (SP05H107) originally consisted of fragments of the femoral head in a mass of faunal ribs and bone fragments, most of the medial and posterior femoral neck which was pushed proximolaterally, and a portion of the proximal diaphysis distal to the juncture of the linea aspera and the spiral line. Most of the lateral surface (~34 mm proximodistally) has been sheared off, such that the only complete contour is right at the distal lesser trochanter. ~27.5 mm of the gluteal tuberosity is preserved in pieces of bone. Subsequent cleaning has removed the mass of broken femoral head and neck pieces and other bone, to leave the diaphyseal section from the distal break (and join with SP05H071A) to the middles of the lesser trochanter and the gluteal tuberosity. Maximum preserved length is 64.0 mm.

Palomas 92pp: Fibula Left

Four pieces of the diaphysis of the left fibula, found near the left foot during excavation. The preserved lengths are 40.0, 58.0, 76.0 and 86.0 mm, for a summed length of ~260 mm. It retains a midshaft section and portions of the distal diaphysis. The elements are variably encased in hard matrix.

Figure S12. The Palomas 92 femoral and fibular remains. Left: posterior view of the left femoral diaphysis. Right: lateral view of the right femur from the distal trochanters to the lateral condyle, with the Palomas 92hh and 92ii pieces placed adjacent to each other at their midshaft contact. Scale bar for the diaphyses: 10 cm. Below left: the approximately midshaft cross-section of the Palomas 92 left fibula (left) and the approximately 65% (mid-proximal) diaphyseal cross-section of its right femur (right); scale bar: 5 cm.

Foot Bones Left

These associated foot bones came out in several breccia blocks, and to varying degrees remain in cemented blocks. The two tarsals, the base of the metatarsal 1, the bases and diaphyses of metatarsals 2 to 4, all of metatarsal 5 and the medial hallucal sesamoid bone are in one unit (SP05H004; Palomas 92a to 92g, 92p). The remainder of the metatarsal 1 (SP05H008) connects to its base. The middle three metatarsal heads are joined in a block with all of the preserved proximal phalanges and the fifth middle phalanx (SP05H005; Palomas 92c to 92f, 92h to 92k, 92n). There are two additional middle phalanges (SP05H007; Palomas 92l & 92m). The lateral one is cemented to a fragment of the metatarsal 2 head (SP05H011; Palomas 92o). The Palomas numbers are by the anatomical bone, even if there is more than one piece for the bone and/or the pieces are joined to more than one cemented unit.

Figure S13. Dorsal view of the Palomas 92 left pedal skeleton remains. Scale bar: 5 cm.

Palomas 92a: Cuboid Left

Complete bone with a vertical crack through the mid-calcaneal facet. Cemented to the lateral cuneiform and metatarsals 4 and 5. Maximum preserved (plantar) length is 30.3 mm.

Palomas 92b: Lateral Cuneiform Left

Complete bone with abrasion to the dorsal navicular facet. Cemented to the cuboid and metatarsals 2 and 3. Maximum preserved length is 18.2 mm.

Palomas 92c: Metatarsal 1 Left

The bone is in two pieces, the lateral base cemented to the plantar metatarsal 2 and the remainder of the bone separate but with a hole in the lateral base. Maximum preserved length is 52.5 mm.

Palomas 92d: Metatarsal 2 Left

The bone consists of the base and the diaphysis with a hole in the medioplantar base. It is cemented to metatarsals 1 and 3, the dorsal half of the head is fused to the metatarsal 3 head and the proximal phalanx 2, and there is a separate fragment of its head. Maximum preserved length is 63.3 mm.

Palomas 92e: Metatarsal 3 Left

The bone consists of the base and the shaft cemented to the lateral cuneiform and the metatarsals 2 and 4, plus the head cemented to the metatarsal 2 and 4 heads and the proximal phalanx 3. Maximum preserved length is 53.9 mm.

Palomas 92f: Metatarsal 4 Left

The bone retains the base and the shaft with a small hole in the dorsal base cemented to the cuboid and the metatarsals 3 and 5, plus the head cemented to the metatarsal 3 head and the proximal phalanx 4. Maximum preserved length is 55.5 mm.

Palomas 92g: Metatarsal 5 Left

Complete bone with distoplantar head abrasion, cemented to the cuboid and the metatarsal 4. Maximum preserved length is 71.3 mm.

Palomas 92h: Proximal Pedal Phalanx 2 Left

Complete bone, cemented to the metatarsal 2 head. Maximum preserved length is 26.5 mm.

Palomas 92i: Proximal Pedal Phalanx 3 Left

Complete bone with dorsal head abrasion, cemented to the metatarsal 3 head and the proximal phalanges 2 and 4. Maximum preserved length is 23.9 mm.

Palomas 92j: Proximal Pedal Phalanx 4 Left

Complete bone with dorsal head abrasion, buried between proximal phalanges 3 and 5 and a fragment of faunal bone. Maximum preserved length is 23.5 mm.

Palomas 92k: Proximal Pedal Phalanx 5 Left

Complete bone, cemented to the metatarsal 5, the proximal phalanx 4 and the middle phalanx 5. Maximum preserved length is 21.1 mm.

Palomas 92l: Middle Pedal Phalanx 2-4 Left

Complete bone with matrix on its base. Maximum preserved length is 13.1 mm.

Palomas 92m: Middle Pedal Phalanx 2-4 Left

Complete bone. Maximum preserved length is 12.9 mm.

Palomas 92n: Middle Pedal Phalanx 5 Left

Complete bone with lateral head abrasion, cemented to the proximal phalanx 5. Maximum preserved length is 8.7 mm.

Palomas 92o: Lateral Hallucal Sesamoid Bone Left

Complete bone, cemented to a metatarsal 2 head fragment. Maximum preserved length is 10.5 mm.

Palomas 92p: Medial Hallucal Sesamoid Bone Left

Complete bone, cemented between the metatarsals 3 and 4. Maximum preserved length is 9.2 mm.

Figure S14. Dorsal (left) and plantar (right) views of the Palomar 92 pedal phalanges. Given fossilization cementation, the proximal phalanx 2 is in approximately lateral view in both views. Scale bar: 5 cm.

Age-at-Death

All of the epiphyses, of the hand and foot bones, of the femora, and of the right elbow, are fully fused, and there is no evidence of the fusion lines for those epiphyses. Palomas 92 was therefore fully mature. However, the ventral sacrum exhibits little or no fusion of the sacral bodies. This is readily apparent between S1 and S2, and it appears to have been the case between S2 and S3 and between S3 and the missing S4. According the system of Belcastro et al. (2008), the degrees of fusion represent stages 0 (unfused) or 1 (<50% fused). With reference to recent European samples, this provides an age-at-death estimate in the mid-third decade for males and slightly younger for females (Belcastro et al., 2008). A mixed Euroamerican and Afroamerican male sample (McKern and Stewart, 1957) provides a similar age range. The Palomas 92 sacrum therefore indicates a young adult age-at-death.

IV. MORPHOMETRIC DATA FOR THE PALOMAS POSTCRANIA

All of the measurements are in millimeters unless otherwise indicated. Measurements with minor estimation are in parentheses. M-# refers to the equivalent number in the Martin system (Bräuer, 1988). Measurements, even if estimated, are provided to the nearest 0.1 mm.

The cross-sectional parameters provided were determined from natural (fossilization) breaks of the diaphyses, the ones sufficiently perpendicular to the diaphyseal axis and with minimal damage so as to permit accurate representations of the cross-sections. Scaled photographs of them were projected enlarged onto a Summagraphics 1812 tablet, and the cross-sectional parameters calculated using SLICE/SLCOMM (Nagurka and Hayes, 1980; Eschman, 1992). The values are the averages of three digitizations. In cases in which the axial orientation of the bone is approximate given the absence of the relevant epiphysis, the anatomically oriented second moments of area (I_x and I_y) are in parentheses. Areas are provided to the nearest 0.1 mm^2; second moments of area are to the nearest mm^4.

Table S3. Morphometrics of the vertebral remains, in millimeters and degrees.

	Palomas 8 C2	Palomas 9 C2	Palomas 92 T12
Cranial facet angle[1]	--	--	right: 85° lateral left: 87° lateral
Caudal facet angle[1]	--	--	right: 34° left: 43°
Cranial facets external breadth	--	--	31.8
Cranial facets internal breadth	--	--	12.4
Caudal facets external breadth	--	--	28.2
Caudal facets internal breadth	--	--	17.0
Cranial body depth (M-4)	--	--	(24.0)
Caudal body depth (M-5)	12.0	--	(25.6)
Cranial body breadth (M-7)	--	--	32.0
Caudal body breadth (M-8)	17.8	--	(33.1)
Body middle height (M-3)	--	--	(20.5)
Lateral body height	15.0	15.5	
C2 maximum ventral height	--	30.3	
C2 mid body height	--	29.3	
C2 dens height	--	14.8	
C2 dens breadth	--	8.5	
C2 dens depth	--	9.3	
Canal cranial breadth	--	--	18.0

[1] The facet angles are relative to the sagittal plane.

Table S4. Ventral body heights of the Palomas 92 sacrum.

S2 ventral height	22.0
S3 ventral height	17.5
S4 ventral height	15.0

Table S5. Diameters of the Palomas 63 right first rib at the mid-diaphyseal curve.

Mediolateral diameter	12.6
External craniocaudal thickness	5.7

Table S6. Measurements and discrete traits of the Palomas humeri.

	Palomas 16	Palomas 17	Palomas 32 Immature	Palomas 92
	Left	Left	Right	Right
Head ant-post diameter (M-10)	--	--	25.5[1]	--
Head med-lat diameter	--	--	32.2[1]	--
Surgical neck maximum diameter	--	--	18.3	--
Surgical neck minimum diameter	--	--	12.2	--
Midshaft maximum diameter (M-5)	19.8	--	--	--
Midshaft minimum diameter (M-6)	14.3	--	--	--
Pectoralis major breadth	≥7.6	--	--	--
Deltoid tuberosity breadth	(8.5)	--	--	--
Mid-dist diaph ant-post diameter	--	--	--	17.6
Mid-dist diaph med-lat diameter	--	--	--	18.7
Mid-dist diaph circumference	--	--	--	61.0
Midshaft cortical thick – anterior	5.5	--	--	--
Midshaft cortical thick – posterior	3.8	--	--	--
Midshaft cortical thick – medial	3.6	--	--	--
Midshaft cortical thick – lateral	3.4	--	--	--
Mid-dist cortical thick – posterior	--	--	--	5.2
Mid-dist cortical thick – anterior	--	--	--	6.0
Mid-dist cortical thick – ant-med	--	--	--	4.9
Mid-dist cortical thick – ant-lat	--	--	--	4.8
Epicondylar breadth (M-4)	--	--	--	58.0
Distal articular breadth (M-12a)	--	--	--	(38.8)
Medial trochlear ant-post dia (M-13)	--	--	--	21.7
Mid min trochlear ant-post dia (S-2)[2]	--	13.2	--	(11.6)
Olecranon fossa breadth (M-14)	--	--	--	28.3

Table S6 (cont.). Measurements and discrete trait of the Palomas humeri.

	Palomas 16	Palomas 17	Palomas 32 Immature	Palomas 92
	Left	Left	Right	Right
Medial pillar thickness (S-12)	--	--	--	7.7
Lateral pillar thickness (S-13)	--	--	--	13.6
Septal aperture	--	--	--	present
Septal aperture prox-dist diameter	--	--	--	((7.0))
Septal aperture med-lat diameter	--	--	--	(8.6)

[1] Epiphyseal diameters.
[2] S-# refers to the equivalent measurement in Senut (1981).

Table S7. Cross-sectional parameters for the Palomas humeri at the specified locations, digitized from a scaled photograph of the distally (Palomas 16) and proximally (Palomas 92) facing diaphyseal breaks. The Palomas 16 axial orientation is approximate, and hence I_x and I_y are in parentheses; the Palomas 92 orientation is based on the distal articulation.

	Palomas 16 ~50%	Palomas 92 ~35%
Total area (mm^2)	242.9	264.4
Cortical area (mm^2)	186.4	233.0
Anteroposterior second moment of area (mm^4) (I_x)	(6591)	5823
Mediolateral second moment of area (mm^4) (I_y)	(3068)	5544
Maximum second moment of area (mm^4) (I_{max})	6593	5834
Minimum second moment of area (mm^4) (I_{min})	3066	5533
Polar moment of area (mm^4) (J / I_p)	9659	11367

Table S8. Measurements of the Palomas 92 right ulna.

Olecranon height (M-7)	21.2
Coronoid height (S-3)	26.3
Head breadth (MCH-3)[1]	15.2
Distal minimum shaft anteroposterior diameter	8.5
Distal minimum shaft mediolateral diameter	8.6

[1] MCH-# refers to the equivalent measurement in McHenry et al. (1976).

Table S9. Measurements of the Palomas 64 and 92 radii.

	Palomas 64	Palomas 92
Head diameter (~anteroposterior) (M-5(1))	--	19.9
Neck anteroposterior diameter (M-5(2))	--	9.7
Neck mediolateral diameter (M-4(2))	--	10.3
Tuberosity length (S-1)	20.8	--
Tuberosity breadth (S-4)	13.3	--
Tuberosity projection (S-8)	16.1	--
Tuberosity position	2[1]	--
Proximal shaft anteroposterior diameter	12.7	--
Proximal shaft mediolateral diameter	11.9	--
Proximal shaft circumference	39.5	--

[1] Anteromedial, following Trinkaus and Churchill (1988).

Table S10. Cross-sectional parameters of the Palomas 64 mid-proximal diaphysis. They are from a scaled photograph of the distal break, at aproximately the mid-proximal diaphysis. The values delete ("original") and then include a bony growth into the medullary cavity from the anteromedial endosteal surface (Fig. S6). Axial orientation is based on the interosseus crest.

	Estimated original	With medullary bony growth
Total area (mm^2)	110.0	110.0
Cortical area (mm^2)	83.3	96.7
Anteroposterior second moment of area (mm^4) (I_x)	813	871
Mediolateral second moment of area (mm^4) (I_y)	979	1030
Maximum second moment of area (mm^4) (I_{max})	989	1031
Minimum second moment of area (mm^4) (I_{min})	803	870
Polar moment of area (mm^4) (J / I_p)	1792	1901

Table S11. Measurements of the Palomas 92 left trapezium and trapezoid bones. Martin numbers are provided for the trapezium and then the trapezoid, as appropriate.

	Trapezium	Trapezoid
Maximum length (M-1)		9.5
Maximum breadth (M-2)	20.1	10.4
Maximum height (M-3)	12.5	9.6
Maximum thickness	(11.9)	
Dorsal breadth	16.7	
Metacarpal articular height (--; M-11c)	11.0	14.5
Metacarpal articular breadth (M-4; M-10c)	(15.6)	10.5 (dorsal)
Metacarpal articular height subtense[1]	3.7	
Metacarpal articular height subtense position[1]	2.7	
Scaphoid articular height (M-5a)	9.5	12.4
Scaphoid articular breadth (M-6; M-4c)	11.6	9.3
Trapezoid articular height (M-9)	7.8	
Trapezium articular height (M-7c)		13.7
Trapezium articular breadth (M-6c)		8.4
Capitate articular height (M-9c)		13.4
Capitate articular breadth (M-8c)		5.3
Scaphoid-trapezoid articular angle	(129°)	
Trapezium tubercle length	(9.6)	
Trapezium tubercle thickness	2.9	
Trapezium tubercle projection	3.3	

[1] Maximum subtense from the metacarpal articular height to the most distal projecting point on the mid-metacarpal 1 facet, plus the position of that subtense along the height chord from the dorsal margin of the facet (Trinkaus, 1989).

Table S12. Measurements of the Palomas 15 and 92 metacarpal bones.

	Palomas 15 Metacarpal 2	Palomas 92 Metacarpal 2	Palomas 92 Metacarpal 4	Palomas 92 Metacarpal 5
Midshaft height	9.6	--	6.4	6.0
Midshaft breadth	7.2	--	6.3	6.3
Head height	13.0	12.5	12.3	--
Head dorsal breadth	13.5	(12.8)	--	--
Head palmar breadth	13.5	(13.5)	11.5	--

Table S13. Midshaft cross-sectional parameters of the Palomas 15 and 92 metacarpals, from scaled photographs of natural breaks. Orientations are based on the metacarpal heads. Palomas 92r has required minor estimation of the damaged subperiosteal contour.

	Palomas 15 Metacarpal 2	Palomas 92 Metacarpal 4
Total area (mm^2)	47.2	(32.2)
Cortical area (mm^2)	37.9	(30.5)
Anteroposterior second moment of area (mm^4) (I_x)	209	(90)
Mediolateral second moment of area (mm^4) (I_y)	141	(77)
Maximum second moment of area (mm^4) (I_{max})	213	(93)
Minimum second moment of area (mm^4) (I_{min})	136	(74)
Polar moment of area (mm^4) (J / I_p)	350	(167)

Table S14. Measurements of the Palomas 92 proximal manual phalanges.

	Palomas 92 Proximal phalanx 3	Palomas 92 Proximal phalanx 4	Palomas 92 Proximal phalanx 5
Maximum length (M-3)	41.0	39.0	--
Articular length	40.2	--	--
Shaft height	6.4	--	7.0
Shaft breadth	10.0	9.0	8.4
Proximal max height	(11.5)	--	10.0
Proximal max breadth	15.1	13.5	--
Prox articular height	(10.5)	--	--
Prox articular breadth	12.9	--	--
Distal height	6.8	--	--
Distal breadth	(11.5)	--	--

Table S15. Measurements of the Palomas middle and distal manual phalanges.

	Palomas 65 Middle 2-4	Palomas 28 Distal 2-4	Palomas 92 Middle 3	Palomas 92 Middle 4	Palomas 92 Distal 3
Maximum length	23.1	19.5	25.6	--	--
Articular length	21.9	17.5	(24.4)[1]	--	--
Midshaft height	5.8	4.1	5.8	--	--
Midshaft breadth	8.3	6.1	8.7	--	--
Proximal max height	10.4	7.5	--	--	--
Proximal max breadth	14.4	12.1	13.4	(12.0)	11.2
Proximal artic height	8.8	6.5	--	--	--
Proximal artic breadth	13.6	10.7	--	--	--
Distal height	6.1		5.5	--	
Distal max breadth	12.1	9.7	10.4	--	--
Distal artic breadth	11.5			--	

[1] The articular length of the Palomas 92 middle manual phalanx 3 was estimated from its maximum length using a least squares regression based on Late Pleistocene middle phalanges 2 – 4 (N = 32) (ArtLen = 0.880 x MaxLen + 1.9; $r^2 = 0.979$; Palomas 92 articular length: 24.4 ± 0.4; $SE_{est} = 1.6\%$).

Table S16. Measurements of the Palomas 52 and 92 femora. Proximodistal locations of diaphyseal diameters are approximate, given the preservation of the femora. Palomas 52 may be immature, given its small dimensions. Palomas 92 is mature despite its small dimensions.

	Palomas 52 left	Palomas 77 --	Palomas 92 right	Palomas 92 left
Maximum length (M-1)	--	--	(397.0)[1]	--
Bicondylar length (M-2)	--	--	(394.0) [1]	--
Biomechanical length[2]	--	--	(372.0) [1]	--
Femur head ant-post diameter (M-19)	--	45.6	(44.2)[3]	--
Femur head sup-inf diameter (M-18)	--	--	(44.3)[3]	--
Gluteal tuberosity breadth	--	--	(10.5)	10.2
Subtrochanteric ant-post diameter (M-10)	19.2	--	--	--
Subtrochanteric med-lat diameter (M-9)	25.5	--	--	--
Mid-proximal anteroposterior diameter	21.1	--	28.2	--
Mid-proximal mediolateral diameter	23.1	--	25.2	--
~Midshaft anteroposterior diameter (M-6)	(19.0)	--	--	--
~Midshaft mediolateral diameter (M-7)	(21.8)	--	--	--
Lateral condylar depth (M-22)	--	--	(60.0)[3]	--

Table S16 Notes

[1] Femoral lengths were estimated using the preserved portions of the right femur. From the distal lesser trochanter to the distal end of Palomas 92mm is 141 mm. By lining up the linea aspera of Palomas 92mm with the linea aspera of Palomas 92nn, the best fit is of the anterolateral extension of Palomas 96mm is along an irregular proximal break of Palomas 92nn. The proximal edge of Palomas 96nn has thin matrix on it, but it provides a good contact for a minimal length estimate for the bone. From the contact point on the proximal break of Palomas 92nn to the distal lateral condyle is 165 mm. Minus 1 mm for the expansion crack gives 164 mm. Added to the proximal piece provides a length of 305 mm from the distal lesser trochanter to the distal lateral condyle (the "SP92Len").

A sample of recent human femora plus three Late Pleistocene femora (N = 40) provides least squares estimates of:

Biomechanical length = (1.12 x SP92Len) + 31.4; $r^2 = 0.901$; Palomas 92 Biomech Len: 372.3 ± 9.7; SE_{est}: 2.6%.

Bicondylar length = (1.17 x SP92Len) + 37.3; $r^2 = 0.900$; Palomas 92 Bicond Len: 393.9 ± 10.2; SE_{est}: 2.6%.

Maximum length = (1.17 x SP92Len) + 40.7; $r^2 = 0.902$; Palomas 92 Max Len: 397.0 ± 10.0; SE_{est}: 2.5%.

[2] The distance from the proximal neck to the average of the distal condyles measured parallel to the diaphyseal axis.

[3] The lateral condyle depth of Palomas 99nn measures 59.5 mm, and it sustained only trivial marginal erosion. It is therefore rounded off to 60 mm. The anteroposterior and superoinferior diameters of the femoral head were estimated from the lateral condylar depth (posterior lateral condyle to anterior lateral patellar surface margin; 60 mm) using least squares regressions based on a pooled recent human (N = 41) and Late Pleistocene fossil human (N = 6) sample. Anteroposterior diameter = 0.641 x LatCondDep + 5.8, $r^2 = 0.881$; estimated diameter: 44.2 ± 1.6 mm; $SE_{est} = 3.6\%$. Superoinferior diameter = 0.620 x LatCondDia + 7.1, $r^2 = 0.849$; estimated diameter: 44.3 ± 1.8; $SE_{est} = 4.1\%$.

Table S17. Cross-sectional geometric parameters of the Palomas 52 left femur and the Palomas 92 right femur, each at approximately 65% (mid-proximal) of the biomechanical lengths of the bones. Orientations are based on placing the linea aspera mid-posterior.

	Palomas 52	Palomas 92
Total area (mm^2)	386.1	534.4
Cortical area (mm^2)	326.9	454.2
AP second moment of area (mm^4)	11800	25935
ML second moment of area (mm^4)	11423	19222
Maximum second moment of area (mm^4)	12294	26499
Minimum second moment of area (mm^4)	10929	18657
Polar moment of area (mm^4)	23223	45157

Table S18. Osteometric and cross-sectional dimensions of the Palomas 13 and 92 left fibulae at approximately midshaft. I_x and I_y are not included since the orientations of the cross-sections are approximate.

	Palomas 13	Palomas 92
Midshaft maximum diameter (M-2)	14.6	12.9
Midshaft minimum diameter (M-3)	10.7	10.2
Midshaft total area (mm^2)	102.6	100.2
Midshaft cortical area (mm^2)	93.7	91.2
Midshaft maximum second moment of area (mm^4)	1137	933
Midshaft minimum second moment of area (mm^4)	647	734
Polar moment of area (mm^4)	1784	1667

Table S19. Measurements of the Palomas 92 cuboid and lateral cuneiform bones.

Cuboid left		Lateral Cuneiform	
Plantar maximum length	30.3	Maximum height	23.7
Dorsal mid articular length	21.7	Navicular articular height	16.2
Dorsal lateral articular length	12.0	Dorsal length (M-1)	18.2
Dorsal medial articular length	20.6	Maximum breadth	13.7
Maximum height	25.8		

Table S20. Measurements of the Palomas 92 left metatarsal bones.

	MT-1	MT-2	MT-3	MT-4	MT-5
Maximum length (M-1)	--	(72.0)	--	--	71.3
Mid articular length	52.5	68.8	--	--	65.2
Medial articular length					60.7
Lateral articular length					66.3
Shaft height (M-4)	--	8.8	--	--	10.0
Shaft breadth (M-3)	--	7.2	--	--	7.5
Proximal max height	--	20.1	--	--	--
Proximal max breadth	--	15.6	12.0	15.6	--
Tuberosity height					15.3
Torsion angle			--	--	(10°)

Table S21. Measurements of the Palomas 92 proximal pedal phalanges.

	PP-2	PP-3	PP-4	PP-5
Maximum length	26.5	23.9	23.5	21.1
Articular length (M-1a)	24.4	21.6	(20.1)	19.0
Shaft height (M-3)	6.1	5.9	--	5.5
Shaft breadth (M-2)	7.1	6.8	(7.0)	(6.8)
Proximal max height (M-3a)	10.5	--	--	10.4
Proximal max breadth (M-2a)	11.6	--	--	--
Proximal artic height	--	--	--	9.4
Proximal artic breadth	--	--	--	(9.0)
Distal height	6.0	--	--	6.4
Distal breadth	8.9	9.1	--	9.7

Table S22. Measurements of the Palomas 67 and 92 middle pedal phalanges.

	Palomas 67 MP-2-4	Palomas 92l MP-2-4	Palomas 92m MP-2-4	Palomas 92n MP-5
Maximum length	15.5	12.9	13.1	8.7
Articular length	12.8	12.4	12.3	8.2
Shaft height	6.2	(3.4)	4.4	3.8
Shaft breadth	9.4	6.5	6.6	8.4
Proximal maximum height	10.4	8.0	7.4	6.7
Proximal maximum breadth	12.2	9.9	9.8	9.8
Proximal articular height	8.6	5.6	5.9	--
Proximal articular breadth	11.6	8.4	9.1	--
Distal height	5.8	3.6	4.0	4.2
Distal breadth	6.1	8.2	8.5	8.6

Table S23. Measurements of the Palomas 92 hallucal sesamoid bones.

	Medial	Lateral
Length	9.2	10.5
Breadth	6.5	7.0
Thickness	--	4.5

Table S24. Measurements of the Palomas 66 and 86 immature pedal proximal phalanges.

	Palomas 66	Palomas 86
Maximum intermetaphyseal length	15.0	--
Midshaft height	3.8	3.6
Midshaft breadth	5.0	5.9
Proximal metaphyseal breadth	8.7	--
Distal height	4.1	--
Distal breadth	6.8	--

V. PALEOPATHOLOGY OF THE PALOMAS POSTCRANIA

Palomas 92 and the isolated postcranial remains from the Sima de las Palomas are remarkably free of pathological lesions. This may be due in part to the dearth of preserved articulations that might reveal osteoarthritis, the young adult age-at-death of Palomas 92, and the presence of immature remains in the sample. Yet, there is no evidence of either trauma or periosteal reactions. None of the muscular insertions reveal enthesopathies.

The only possibly pathological alteration is the bony growth into the mid-proximal medullary cavity of the Palomas 64 radius (Fig. S6). Its etiology is unclear, and it does not appear to have affected the subperiosteal bone.

VI. COMPARATIVE SAMPLES IN THE QUANTITATIVE ANALYSES

Neandertals (MIS 4-3)
Amud, La Chapelle-aux-Saints, Combe Grenal, Feldhofer, La Ferrassie, Fond-de-Forêt, Kebara, Kiik-Koba, Lezetxiki, Oliveira, La Quina, Regourdou, Saint-Césaire, Shanidar, El Sidrón, and Spy

Middle Paleolithic Modern Humans (MIS 6-5)
Qafzeh and Skhul

Early Upper Paleolithic Modern Humans (MIS 3)
Brassempouy, Mladeč and Nazlet Khater

Mid Upper Paleolithic Modern Humans (MIS 3)
Arene Candide, Barma Grande, Bausu da Ture, Caviglione, Cro-Magnon, Dolní Věstonice, Grotte-des-Enfants, Nahal-ein-Gev, Paglicci, Pataud, Paviland, Pavlov, Předmostí, La Rochette, Sunghir, and Veneri

Early Neandertals (MIS 5)
Krapina, Tabun

SI LITERATURE CITED

Belcastro MG, Rastelli E, Mariotti V. 2008. Variation in the degree of sacral vertebral body fusion in adulthood in two European modern skeleton collections. Am J Phys Anthropol 135:149-160.

Bräuer G. 1988. Osteometrie. In: Knussman R editor, Anthropologie I. Stuttgart: Fischer Verlag. p 160-232.

Eschman PN. 1992. SLCOMM Version 1.6. Albuquerque: Eschman Archeological Services.

McHenry HM, Corruccini RS, Howell FC. 1976. Analysis of an early hominid ulna from the Omo Basin, Ethiopia. Am J Phys Anthropol 44:295-304.

McKern TW, Stewart TD. 1957. Skeletal age changes in young American males analyzed from the standpoint of age identification. Headquarters Quartermaster Research and Development Command Technical Report EP-45:1-179.

Nagurka ML, Hayes WC. 1980. An interactive graphics package for calculating cross-sectional properties of complex shapes. J Biomech 13:59-64.

Pyle SI, Waterhouse AM, Greulich WW. 1971. A Radiographic Standard of Reference for the Growing Hand and Wrist. Cleveland: Case Western Reserve University Press.

Ruff CB. 2010. Structural analyses of postcranial skeletal remains. In: Morgan ME, editor. Pecos Pueblo Revisited: The Biological and Social Context. Pap Peabody Mus 85:93-108.

Ruff CB, Walker A, Trinkaus E. 1994. Postcranial robusticity in *Homo*, III: Ontogeny. Am J Phys Anthropol 93:35-54.

Scheuer L, Black S. 2000. Developmental Juvenile Osteology. London: Academic Press.

Senut B. 1981. L'Humérus et ses Articulations chez les Hominidés Plio-Pleistocènes. Paris: CNRS.

Trinkaus E. 1989. Olduvai Hominid 7 trapezial metacarpal 1 articular morphology: Contrasts with recent humans. Am J Phys Anthropol 80:411-416.

Trinkaus E, Churchill SE. 1988. Neandertal radial tuberosity orientation. Am J Phys Anthropol 75:15-21.

Walker MJ, Gibert J, López MV, Lombardi AV, Pérez-Pérez A, Zapata J, Ortega J, Higham T, Pike A, Schwenninger JL, Zilhão J, Trinkaus, E. 2008. Late Neandertals in southeastern Iberia: Sima de las Palomas del Cabezo Gordo, Murcia, Spain. Proc Natl Acad Sci USA 105:20631-20636.